frontiers | Frontiers in Ecology and Evolution

TYPE Original Research
PUBLISHED 19 May 2023
DOI 10.3389/fevo.2023.1173341

OPEN ACCESS

EDITED BY
Stergios D. Zarkogiannis,
University of Oxford, United Kingdom

REVIEWED BY
George Lyras,
National and Kapodistrian University of Athens, Greece
Emmanuel Paul Gilissen,
Royal Museum for Central Africa, Belgium
Alejandro Pérez Ramos,
Malaga University, Spain

*CORRESPONDENCE
Saverio Bartolini-Lucenti
✉ saverio.bartolinilucenti@unifi.it
Lorenzo Rook
✉ lorenzo.rook@unifi.it

RECEIVED 24 February 2023
ACCEPTED 24 April 2023
PUBLISHED 19 May 2023

CITATION
Frosali S, Bartolini-Lucenti S, Madurell-Malapeira J, Urciuoli A, Costeur L and Rook L (2023) First digital study of the frontal sinus of stem-Canini (Canidae, Carnivora): evolutionary and ecological insights throughout advanced diagnostic in paleobiology.
Front. Ecol. Evol. 11:1173341.
doi: 10.3389/fevo.2023.1173341

First digital study of the frontal sinus of stem-Canini (Canidae, Carnivora): evolutionary and ecological insights throughout advanced diagnostic in paleobiology

Samuele Frosali[1], Saverio Bartolini-Lucenti[1,2]*, Joan Madurell-Malapeira[1,3], Alessandro Urciuoli[2,4,5], Loïc Costeur[6] and Lorenzo Rook[1,7]*

[1]Department of Earth Science, University of Florence, Florence, Italy, [2]Institut Català de Paleontologia Miquel Crusafont, Universitat Autònoma de Barcelona, Cerdanyola del Vallès, Spain, [3]Department of Geology, Universitat Autònoma de Barcelona, Cerdanyola del Vallès, Spain, [4]Universitat Autònoma de Barcelona, Cerdanyola del Vallès, Spain, [5]Division of Palaeoanthropology, Senckenberg Research Institute and Natural History Museum Frankfurt, Frankfurt am Main, Germany, [6]Naturhistorisches Museum Basel, Basel, Switzerland, [7]Changes Foundation, Sapienza Università di Roma, Roma, Italy

Introduction: The phylogenetic and ecological importance of paranasal sinuses in carnivorans was highlighted by several previous authors, mostly in extant species. Nevertheless, no specific study on this feature on extant canids, and no one on fossil representatives of the family, has been published up to now. Here, we analyze for the first time the paranasal sinus of extant and fossil canids through computed tomographic techniques to characterize them morphologically and morphometrically, making ecological inferences.

Methods: To do so, we applied for the first time an innovative deformation-based morphometric approach.

Results: The results obtained for extant species highlight a remarkable correlation between morphology and ecomorphotypes previously defined by some scholars (namely hypercarnivorous group-hunters; small-prey hypercarnivores, mesocarnivores, hypocarnivores). Our results thus support the direct relationship between diet preferences and the development of frontal sinus in canids. Regarding fossil specimens, we reconstructed for the first time the frontal sinus of three *Eucyon* species and compared it to those of living forms.

Discussion: The best-preserved specimen, the only known cranium of *Eucyon adoxus* dated to the Late Pliocene of Saint-Estève (France), displayed similarities with hypercarnivorous group-hunter canids by the large sinus prominences. Given that the overall craniodental morphology of *E. adoxus* suggests that it acted as a small prey hypercarnivore—similar to extant *Canis simensis*—the aforementioned affinities might have evolved independently, in relation to high stresses during feeding. Overall, our study demonstrates that morphological inspection and deformation-based geometric morphometrics complement each other and allow a thorough investigation of sinus shape variability, thus enabling the study of sinus morphology in other fossil carnivorans with the ultimate goal of inferring their ecological preferences.

KEYWORDS

innovative morphometrics, sustainable cultural heritage, Canidae, paranasal sinuses, paleoecology, *Eucyon*

1. Introduction

1.1. Dispersal of the tribe Canini in Eurasia

Currently, the members of the family Canidae are widely distributed across Eurasia and Africa, but geologically speaking this is just a recent achievement. Throughout most of their history, the distribution of canids was restricted to North America (Wang and Tedford, 2008; Tedford et al., 2009; Sotnikova and Rook, 2010). The major biotic events related to the dispersal of the subfamily Caninae (to which all extant canids belong to) and their evolution in Eurasia coincided with faunal turnovers that, in these continents, occurred between 5.5 and 0.5 Ma. One of the two major events of the Canini dispersal in Eurasia was the "*Eucyon* event" (*sensu* Sotnikova and Rook, 2010) that took place at the end of the Miocene (the other main event was the so-called "*Canis* event" at the beginning of the Late Pliocene; Sotnikova and Rook, 2010). Species of the genus *Eucyon* (Tedford and Qiu, 1996) indeed appeared in Central Asia, Europe, and Africa by the latest Miocene (Figure 1). For instance, the remarkable Late Miocene occurrences of *Eucyon monticinensis* (Rook, 1992) in Europe, *Eucyon davisi* (Merriam, 1911) in Asia, and *Eucyon intrepidus* (Morales et al., 2005) in Africa, were roughly contemporaneous. The genus then experienced multiple radiations in Eurasia and Africa, reaching a relatively high diversity in the Pliocene of Eurasia (Rook, 2009; Figure 1). The diversification of the Canini in Asia peaked at the beginning of the Early Pliocene, as evidenced by the appearance of *Nurocyon chonokhariensis* (Sotnikova, 2006) and *Eucyon zhoui* (Tedford and Qiu, 1996), and by the increase in number of *E. davisi* finds (Sotnikova and Rook, 2010). The European diversity peaked later with the arrival of "*Canis*" *michauxi* (Martin, 1973), *Eucyon adoxus* (Martin, 1973), and *Eucyon odessanus* (Odintzov, 1967) in the Late Ruscinian (Late Pliocene; Sotnikova and Rook, 2010) (Figure 1). In the Early Pleistocene, after the "*Canis* event," there was a species turnover on the continent and the species of the genus *Eucyon* went almost completely extinct, being limited to the Chinese *Eucyon minor* (Teilhard de Chardin and Piveteau, 1930) and "*Canis*" *kuruksaensis* (Sotnikova, 1989), while *Canis sensu* lato underwent a wide diversification. This turnover included *Canis teilhardi* (Qiu et al., 2004), *Canis longdanensis* (Qiu et al., 2004), *Canis chihliensis* (Teilhard de Chardin and Piveteau, 1930), *Canis* (*Xenocyon*) *brevicephalus* (Qiu et al., 2004), and *Canis* (*Xenocyon*) *dubius* (Teilhard de Chardin, 1940) in China, and the western forms like the renown *Canis etruscus* (Forsyth-Major, 1877), *Canis arnensis* (Del Campana, 1913), *Canis borjgali* (Bartolini-Lucenti et al., 2020), *Canis* (*Xenocyon*) *falconeri* (Forsyth-Major, 1877), and *Canis accitanus* (Garrido and Arribas, 2008; Sotnikova and Rook, 2010). The diversity of the *Canis* s.l. group decreased in the second half of the Early Pleistocene of Eurasia, becoming mostly limited to the large hypercarnivorous form *Canis* (*Xenocyon*) *lycaonoides* (Kretzoi, 1938) and small wolf *Canis mosbachensis* (Soergel, 1925) (and its possible zoogeographic extreme *Canis variabilis* Pei, 1934) (Rook et al., 2023).

1.2. Brief overview of biomechanics of the frontal sinus in carnivorans

The frontal sinus is an often-overlooked anatomical structure. Nevertheless, recent studies unveil the renovated interest for this paranasal cavity in paleontological and paleoanthropological research, for its potential at different levels, e.g., evolutionary, biomechanical, ecological one (Balzeau et al., 2022).

In carnivorans, the first introduction of the frontal sinus as a taxonomic-useful character was proposed by Huxley (1880) and is today widely recognized by the scientific community as a diagnostic feature in the phylogenetic analysis of Canidae. The basal state (lack of the sinus) is manifested externally by a shallow depression or a groove, creasing the dorsal surface of the postorbital process (Tedford et al., 1995): this condition is present in almost all the living species of the tribe Vulpini and it is indeed known as the "vulpine crease." In members of the tribe Canini, this cavity inflates and expands its size: the most derived condition is shown by *Canis*, where the sinus penetrates the postorbital process to its tip and expands posteriorly along the rostrodorsal surface of the braincase, ultimately reaching the frontoparietal suture (Tedford et al., 1995). This enlargement of the frontal region produces a deeply convex morphology of the dorsal surface of the cranium above the orbits and an enlargement, in width, of the postorbital constriction.

Among other cranial features, like dentition morphology or snout length, the development of the frontal sinus is linked to the type of diet the species evolved. Particularly, large canids with hypercarnivorous diets tend to have more developed sinuses and enlarged, domed frontals. In durophagous carnivorans, both in Hyaenidae and Borophaginae, the frontal sinus extends backward toward the posterior tip of the skull and, as a result, there is a large air space between the braincase and the parietal bones above it (Paulli, 1900; Joeckel, 1998; Vinuesa et al., 2015). Werdelin (1989) and Joeckel (1998) proposed that such a domed head in bone-cracking hyaenids and canids serves to transmit the great stresses from the premolars to the back of the skull, thereby reducing the bending stress of the rostrum. The main hypothesis to explain the presence of the frontal sinus in carnivorans is indeed that these structures are useful for the even dissipation of stresses linked to feeding mechanics. Some studies (among others Curtis and Van Valkenburgh, 2014) also pointed out a relationship between the intraspecific variations of the morphology and size of the frontal sinus and the diet of the individual (the softer the food eaten, the smaller the frontal sinus; Curtis et al., 2018; Pérez-Ramos et al., 2020; Ruiz et al., 2023). Other hypotheses have been suggested to explain the function of these structures, among others the idea that frontal sinuses are useful for brain cooling, olfaction, potential sensory enhancement ability, or for the maximization of muscle attachment areas, or even hibernation (Joeckel, 1998; McGreevy et al., 2004; Vinuesa et al., 2015, 2016; Vinuesa, 2018; Pérez-Ramos et al., 2020). However, none of these explanations is entirely satisfactory and one hypothesis does not necessarily exclude another. The present paper offers the first in-depth study of the frontal sinus of extant and fossil canids using computed tomography and innovative 3D methodologies (never applied to these structures) to characterize and analyze them and, eventually, draw ecological inferences on the considered fossil taxa.

2. Materials and methods

2.1. Studied and comparative material

This study reports the first digital analysis of the frontal sinuses of three stem-Canini of the genus *Eucyon*: the only known cranium

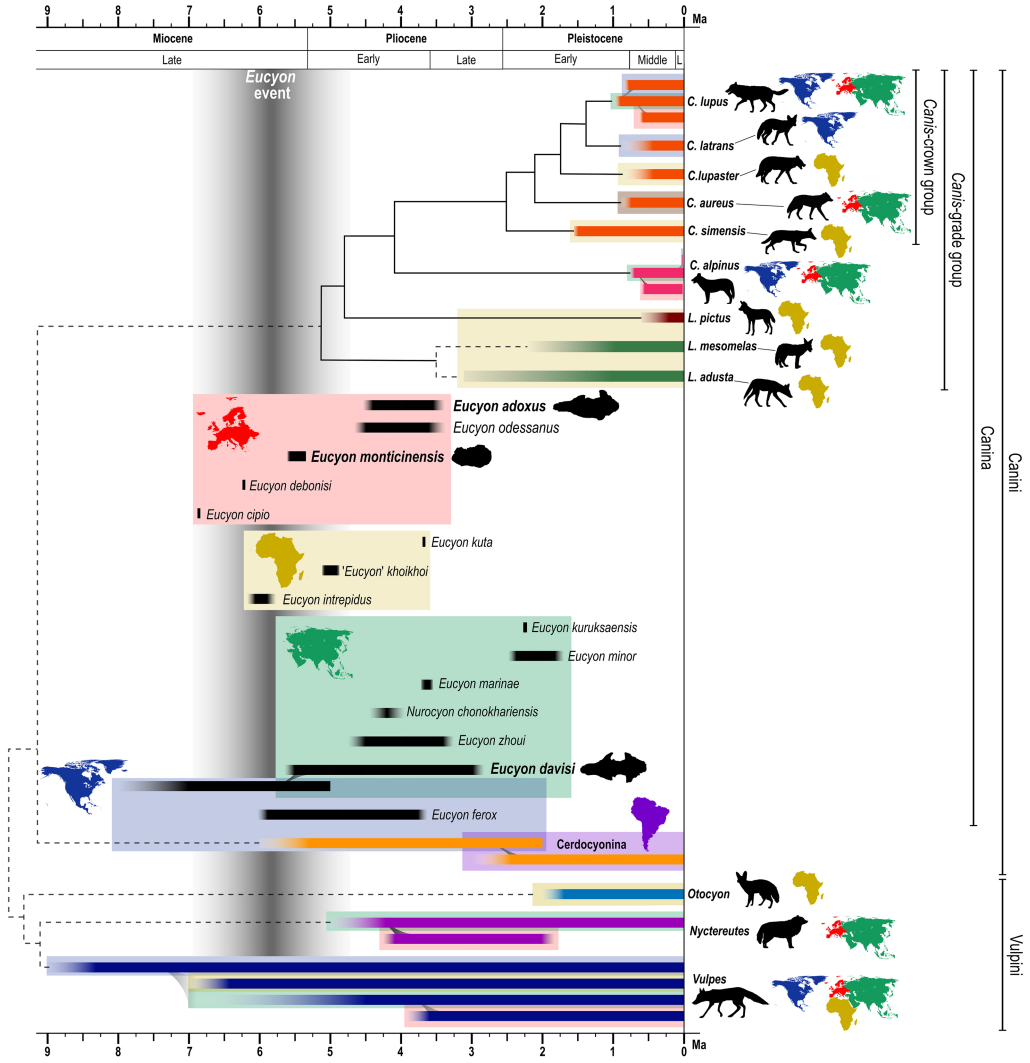

FIGURE 1
Stratigraphic, phylogenetic, and geographical scheme of *Eucyon* spp. in the framework of extant canids evolution and zoogeography from Miocene to modern times. The phylogenetic relationships are compiled using widely accepted and recent molecular and total evidence analyses (e.g., Zrzavý et al., 2018; Perri et al., 2021). Solid lines represent undisputed patterns of affinities; divergence between solid-lines groups are time-calibrated using average time of divergence expressed in these works (e.g., Perri et al., 2021). Dashed lines account for disputed topologies of trees (e.g., paraphyly of *Lupulella*; relationship among Vulpini; *cf.* Wayne and Ostrander, 2007 and Zrzavý et al., 2018). Time of the nodes in the dashed-lined groups should not be taken as significative. Considering the disputed nature of several *Eucyon* spp. (as expressed in the text) we reported only their chronological and geographic distribution. Data are taken from: Tedford and Qiu (1996), Sotnikova (2006), Spassov and Rook (2006), De Bonis et al. (2007), Montoya et al. (2009), Rook (2009), Tedford et al. (2009), Werdelin et al. (2015), Bartolini-Lucenti and Rook (2021), Valenciano et al. (2022). '*Eucyon* event' is taken from Sotnikova and Rook (2010). Colors of the chronological ranges represents clades. Ranges of other canids are taken from previously cited literature and also from: Stiner et al. (2001), Boudadi-Maligne (2010), Werdelin and Sanders (2010), Bartolini-Lucenti et al. (2018), Marciszak et al. (2021), Tamvakis et al. (2022), Martínez-Navarro et al. (2023). Color continents maps next to specific names represent presence of the species in one/more than one continent(s), following the color code of the boxes in the figure.

of the species *Eucyon adoxus*, from the Late Pliocene of Saint-Estève (France; Rook, 2009) and stored at the Natural History Museum of Basel (NMB Rss.45); a cranium (F:AM 97057) of *Eucyon davisi* from the Early-Late Pliocene of Xiakou, Yushe Basin (China; Tedford and Qiu, 1996), currently stored at the American Museum of Natural History of New York (U.S.A.); and, the only known cranial specimen of *Eucyon monticinensis*, from the latest Late Miocene of Cava Monticino (Italy, Bartolini-Lucenti et al., 2022) and stored in the Civic Museum of Natural Sciences of Faenza. The objective of the study is the comparison of the sinus of these fossil species to that of selected extant Canidae. The extant comparative specimens used here are held at the "La Specola" Zoology Museum of Florence (MZUF), the Giacomo Doria Natural History Museum of Genoa (CE) and the Earth Science Department of the University of Florence (DST). Additional specimens were downloaded from the digital repository MorphoSource.[1] The considered comparative sample includes (Supplementary Table S1) four specimens of *Canis lupus*, Linnaeus (1758), four of *Canis lupaster* (Hemprich and Ehrenberg, 1828/1834), three of *Canis simensis* Rüppell (1835/1840), two of *Canis aureus* (Linnaeus, 1758), one of *Canis latrans*

1 www.morphosource.org

Say (1823), one of *Lupulella adusta* (Sundevall, 1847), four of *Lupulella mesomelas* (Schreber, 1775), two of *Lycaon pictus* (Temminck, 1820), and one of *Vulpes lagopus* (Linnaeus, 1758). To compare morphologically and morphometrically the specimens we used the digital analysis of images derived from CT scans via the software Amira (ver. 5.4.5, Thermo Fisher). Tomographic scans of the material from Florence and Faenza were acquired at the Medical Radiology ward ("SOS Radiologia") of the San Giovanni di Dio Hospital (Florence, Italy) using a Siemens Somatom Definition AS scanner. *Eucyon adoxus* was scanned at the Biomaterials Science Center of the University of Basel, Switzerland using a Phoenix Nanotom (GE). The specimen of *Eucyon davisi* was scanned at the University of Texas high-resolution X-ray Computed Tomography Facility (Austin, Texas, U.S.A.). For the specimens downloaded from Morphosource, we report the info included in the metadata and accompanying files of the raw data: m-81.001, *Canis simensis*, originally held at the AMNH Mammal Collection, was scanned by the University of Texas high-resolution X-ray Computed Tomography Facility (Austin, Texas, U.S.A.). 80-50-290, *Canis latrans*, kept at the University of Arkansas Museum and was scanned by the MicroCT Imaging Consortium for Research and Outreach (Fayetteville, Arkansas, U.S.A.). 368.443, *Lycaon pictus* was scanned by the University of Texas high-resolution X-ray Computed Tomography Facility (Austin, Texas, U.S.A.), while the original sample comes from NMNH – Division of Mammals. The data obtained from these images made the reconstruction of the frontal sinuses of all the specimens possible. We decided to use the left sinus only to ease the alignment of the surfaces and, consequently, their analysis with deformation-based geometric morphometric methods.

2.2. Nomenclature and abbreviations

2.2.1. Proposed nomenclature of the frontal sinuses

We propose for the first time a nomenclature to describe the frontal sinus in canids and carnivorans (Figure 2). The sinus is divided into three regions: rostral, caudal, and ventral ones. The rostral and caudal regions are characterized by specific features on their dorsal, medial, lateral, and ventral surfaces. The ventral region is generally described for its medial and lateral sides and its rostral and caudal margins. The features, although variable, can be recognized on the outer surface. Here we report the names and abbreviations for the analyzed specimens. Abbreviations and their definition, in alphabetical order: **ci**, caudal incision (if more than one: medial ci, lateral ci, etc.); **dcll**, dorsocaudal lateral lobe; **dcml**, dorsocaudal medial lobe; **ds**, dorsal sulcus (if the sulcus is simple it may be named "longitudinal ds"; if it branches, it can have "a transverse part of the ds"; etc.); **l**, lobe (a large inflated portion of the sinus), **lb**, lobule (a smaller and less prominent lobe); **p**, prominence (general term to describe an inflation of the surface of the sinus); **pol**, postorbital lobe; **ri**, rostral incision (generally divides the rostral region of the sinus in two sides: the rostrolateral lobe and the rostromedial one); **rll**, rostrolateral lobe; **rml**, rostromedial lobe; **vl**, ventral lobe (the tip of the ventral region); **vlp**, ventrolateral prominence.

2.2.2. Other abbreviations used in the text

List of abbreviations used in the paper, in alphabetical order: BM, body mass; CBL, condylobasal length of the cranium (prosthion-occipital condyles); LmaxS, maximum rostrocaudal length of the frontal sinus; TL, total length of the cranium (measured from prosthion-akrokranion); Vol, volume of the frontal sinuses.

2.2.3. Morphometric variables and ecomorphogroups

We used Autodesk Meshmixer (ver. 3.5.474, Autodesk) and Artec Studio 15 Professional (ver. 15.0.3.425, Artec) software to ameliorate and regularize the mesh structure, as well as to measure the sinus volume (Vol), sinus maximum rostrocaudal length (LmaxS), the cranial length (TL) and the condylobasal length (CBL). The latter was used to estimate the body mass of each specimen, using the regression formula proposed by Van Valkenburgh (1990). Van Valkenburgh and Koepfli (1993), studying extant canids dietary preferences, established four distinct ecological groups. The differed for their morphological features and the proportional amount of vertebrate prey in their diet: Group 1 and 2 have >70% of vertebrate meat in their diet, thus are considered hypercarnivore canids. They are distinguished by the fact that Group 1 canids cooperatively hunt large prey, whereas Group 2 are hypercarnivorous specialized in small prey. Group 3 canids are mesocarnivorous, with an income of 70–50% of vertebrate meat in their diet. Group 4 represent the hypocarnivorous dogs with <50% of meat. We used these well attested groups to investigate the ecological implication of the development of the frontal sinus.

To assess the presence of correlation among the variables considered in the analysis, we performed ordinary least squares (OLS) regressions on natural log-transformed linear variables (ln TL, ln LmaxS, in mm), natural log-transformed cube root of the left sinus volume (ln Vol, in mm^3), and on the natural log-transformed body mass (ln BM, in kg). The regressions were performed for the whole Canidae sample, as well as for two subsets based on ecological preferences (group hunters vs. non-group hunters) due to the difference noted in one of the ecological groups. We also checked the homogeneity of the slopes and intercepts between group hunters and the rest of the sample via analysis of the covariance (ANCOVA). All regressions were performed in R Studio (v. 2023.03.0 + 386 "Cherry Blossom" release 3c53477afb13ab959aeb5b34df1f10c237b256c3, 2023-03-0936; RStudio Team, 2021) for R (v. 4.1.2; R Core Team, 2021) using the lm() function of the base package 'stats', whereas we used the anova() function of the 'car' v. 3.0–11 (Fox and Weisberg, 2019) to perform the ANCOVA.

2.2.4. Diffeomorphic surface matching analyses

To further inspect the shape variation in the canid sinus, we employed a diffeomorphic surface matching (DSM) approach, which is a recently-developed landmark-free geometric morphometrics method that allows the direct comparison between continuous surfaces by relying on their geometrical correspondence (Glaunès and Joshi, 2006; Durrleman et al., 2014). This method takes into account all data points at the same time and does not require point-to-point correspondence, thus allowing the use of surfaces composed by a different number of faces (Durrleman et al., 2012). From an operational viewpoint, DSM first estimates the average shape for the considered sample and identifies its most variable portions, attaching a number of initial control points to them. The deformations from the average to each of the analyzed specimens are then modeled as smooth and invertible functions (that are, diffeomorphisms) and compiled to build an atlas for the entire sample. Compared with

10.3389/fevo.2023.1173341

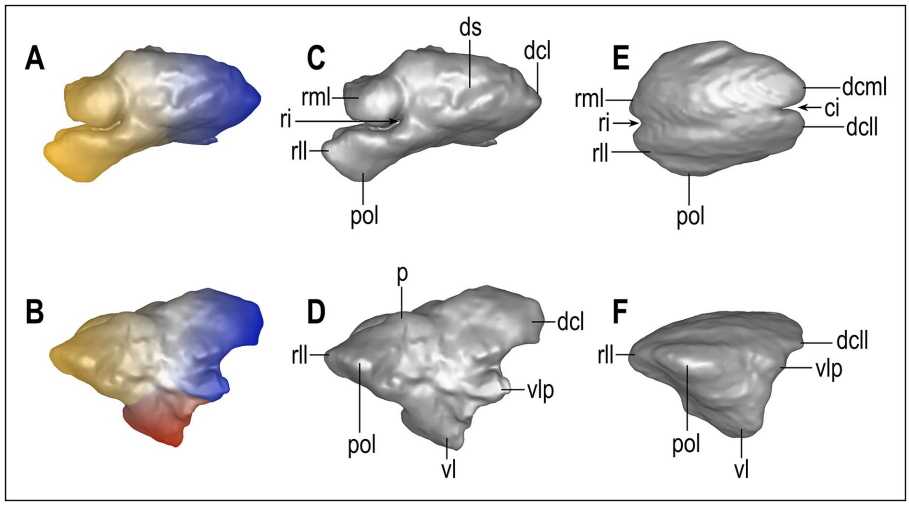

FIGURE 2
Nomenclature of the main parts of the frontal sinus of Canidae. *Eucyon adoxus* (NMB Rss.45, **A–D**) and *C. lupaster* (MZUF-2714, **E,F**) were taken as models because their sinuses represent, respectively, a quite complex and one of the simplest versions of this paranasal structure (not to scale). The color map **(A,B)** represents the principal areas of the sinus: yellow, rostral region; blue, caudal region; red, ventral region. ci, caudal incision; dcll, dorsocaudal lateral lobe; dcml, dorsocaudal medial lobe; ds, dorsal sulcus; l, lobe; lb., lobule; p: prominence; pol, postorbital lobe; ri, rostral incision; rll, rostrolateral lobe; rml, rostromedial lobe; vl, ventral lobe; vlp, ventrolateral prominence.

landmarks, correspondence between surfaces is not strictly homologous, which is particularly convenient for structures with a very complex 3D morphology that does not allow to identify a large number of homologous points, as in the case of frontal sinuses and of other craniodental structures (e.g., semicircular canals and enamel/dentine junction; Urciuoli et al., 2020; Zanolli et al., 2022).

Prior to performing DSM analyses, the surfaces required a number of preparatory steps. First the 3D models of the left sinus of each specimen were decimated to 40,000 triangles (±100 triangles) in Amira and saved in PLY format. Given the complexity and variability of the sinus, the alignment methods used for preprocessing the surfaces in other DSM analyses (Beaudet et al., 2016; Urciuoli et al., 2020) did not yield satisfactory results. To circumvent this issue, we defined a number of landmarks (see Table 1) that allowed us to generally describe its morphology and orientation. The aforementioned landmarks were placed on each individual in Amira software and used to perform a General Procrustes alignment in R using the procSym() function of the 'Morpho' v. 4.1.3 (Schlager, 2017) package. The obtained aligned configurations were then used to extract the rotational matrix and scaling factor for each individual, which were then applied to the corresponding surface using two functions, computeTransform() and applyTransform(), of the 'Morpho' package. The aligned surfaces were then converted into legacy VTK files using the open-source software Paraview v. 5.6.0.[2] The VTK files were then analyzed with Deformetrica ver. 4.3 (Bône et al., 2018) using the 'DeterministicAtlas' analysis with Kernel size = 0.10, resulting in the identification of 7,800 control points. The *V. lagopus* individual was not included in the analysis due to its very reduced sinus morphology. R scripts and data used here for the analyses are available at the following link http://dx.doi.org/10.5281/zenodo.7836886.

TABLE 1 List of landmarks (LM) used in the analysis and their number and definition.

LM number	Definition
1	Rostralmost (Anteriormost) point on the rostromedial lobe.
2	Caudalmost (Posteriormost) point of the incision between rostromedial and lateral lobe.
3	Lateralmost point of the lateral lobe.
4	Medialmost point on the medial side of the sinus.
5	Caudalmost (Posteriormost) point of the sinus.
6	Ventralmost point of the frontal sinus.

The obtained deformation fields (i.e., the output of the DSM analyses) were then inspected with different multivariate methods to identify the possible presence of patterns of shape variation in the data. First, we computed a principal component analysis (PCA), which allows to reduce the high dimensionality of the data and to concentrate the variance in the first axes (components). The resulting components were then used to perform a canonical variate analysis (CVA)—with the CVA() function of the 'Morpho' package—using hunting and dietary preferences (group hunters, hypercarnivory of small prey, and mesocarnivory) as grouping factor, thus enabling us to assess the presence of a group structure within the data. We included only the first seven components (accounting for the 71.9% of total variance) as these returned the best classification results, a practice commonly used in high-dimensional shape data (e.g., Zanolli et al., 2022). The fossil specimens (*E. adoxus* NMB Rss.45, *E. davisi* F:AM 97057) and the hypocarnivore *Lupulella adusta* (MZUF-8496) were plotted *a posteriori* onto the shape space. For these specimens, we also computed cross-validated posterior probabilities and typicality probabilities using their CVA scores. Posterior probabilities assume that an individual must belong to one of the *a priori* defined groups and are expressed as a percentage. In contrast, the interpretation of

2 www.paraview.org

10.3389/fevo.2023.1173341

typicality probabilities is less intuitive, as they test the null hypothesis of group membership for a given specimen and return a *p*-value, which allows to reject the null hypothesis (i.e., the specimen is an outlier for the considered group) at $p < 0.05$. Finally—as for the morphometric variables—we assessed the possible presence of allometric trends in the shape data by regressing each of the obtained PCs and CVs against the log-transformed body mass (in kg) in R.

3. Results

3.1. Description of the sinuses of *Eucyon*

The three species of the genus *Eucyon* considered in this study show quite different morphologies of the frontal sinuses. The cranium of *E. monticinensis* MSF 466, at present the only cranium of the species ever recovered and described, is extremely deformed due to taphonomic processes. The deformation affecting the fossil involved a dorsoventral compression, with a left lateral component, so that the cranium seems to lie on the left side. The left sinus, the only one preserved in MSF 466, is thus heavily deformed (Figure 3). Despite this problematic, the 3D model shows that this species presents quite a small sinus, with reduced lobes. Further comments on its development are hindered by the deformation: it is indeed hard to understand the dorsoventral extension of the sinus, as well as the development of its ventral lobe. The other species of the genus, also shown in Figure 3, show instead a very different morphology of this paranasal cavity. *Eucyon adoxus* possesses instead a well-developed frontal sinus with a marked rostral incision that identifies two prominent rostral lobes. On the dorsal surface, the sinus of *E. adoxus* shows evident prominences along the main axis of the sinus, marked by a dorsal sulcus. The ventral lobe is elongated ventrally, giving the frontal sinus a triangular-like outline, in lateral view. The postorbital lobe is developed, resembling in shape the morphology of the process of the frontal bone: indeed, the sinus visibly invades the whole length of the process (Figure 3). This species shows also a trigonal dorsocaudal lobe and a marked ventrolateral prominence jutting caudally. The sinus of *Eucyon davisi* is rostrocaudally elongated but with fairly inflated generalized structures (Figure 3). The rostrocaudal elongation is remarkable: even if they do not reach the frontoparietal suture, the sinus covers a fair portion of the endocranial cavity. There is no rostromedial lobe, whereas the rostrolateral one is prominent, in dorsal and lateral views (Figure 3). In lateral view, the ventral lobe is slender compared to the inflated and rounded dorsocaudal lobe. The postorbital lobe is reduced and sharp, jutting pointily on the lateral plane.

3.2. Morphological and morphometric comparison of the frontal sinuses in Canidae

Figure 4 shows the final reconstruction of the frontal sinuses of a single specimen for each fossil and extant species, considered in

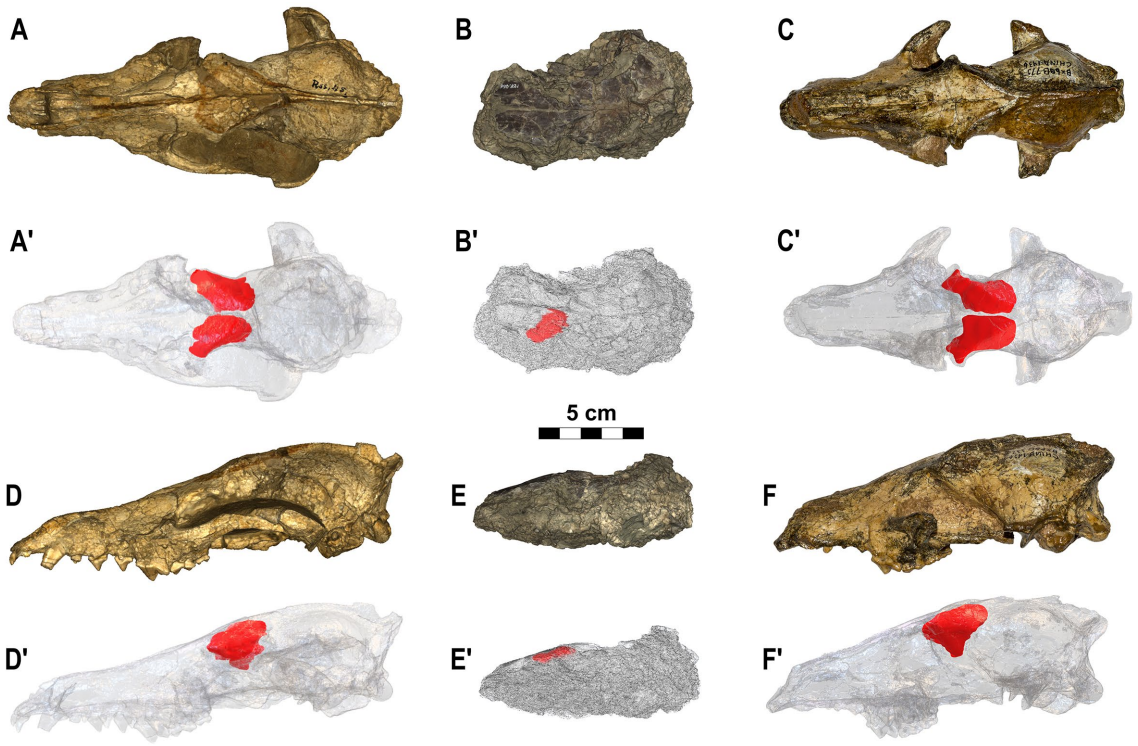

FIGURE 3
Crania of the three species of *Eucyon* here analyzed. **(A–A',D–D')** *Eucyon adoxus* (NMB Rss.45) from St. Estève (Late Pliocene, MN 15; southern France), in dorsal **(A–A')** and in left lateral **(D–D')** views. **(B–B',E-E')** *Eucyon monticinensis* (MSF 466) from Cava Monticino (latest Miocene, 5.61–5.33 Ma; Emilia-Romagna, Italy), in dorsal **(B–B')** and left lateral **(D–D')** views. **(C–C',F-F')** *Eucyon davisi* (F:AM 97057) from near Xiakou (late Early-Late Pliocene, ~4.0–3.0 Ma; Yushe Basin, Shanxi, China), in dorsal **(C–C')** and left lateral **(F–F')** views. **(A'–F')** Highlight the position of the frontal sinuses within the crania.

10.3389/fevo.2023.1173341

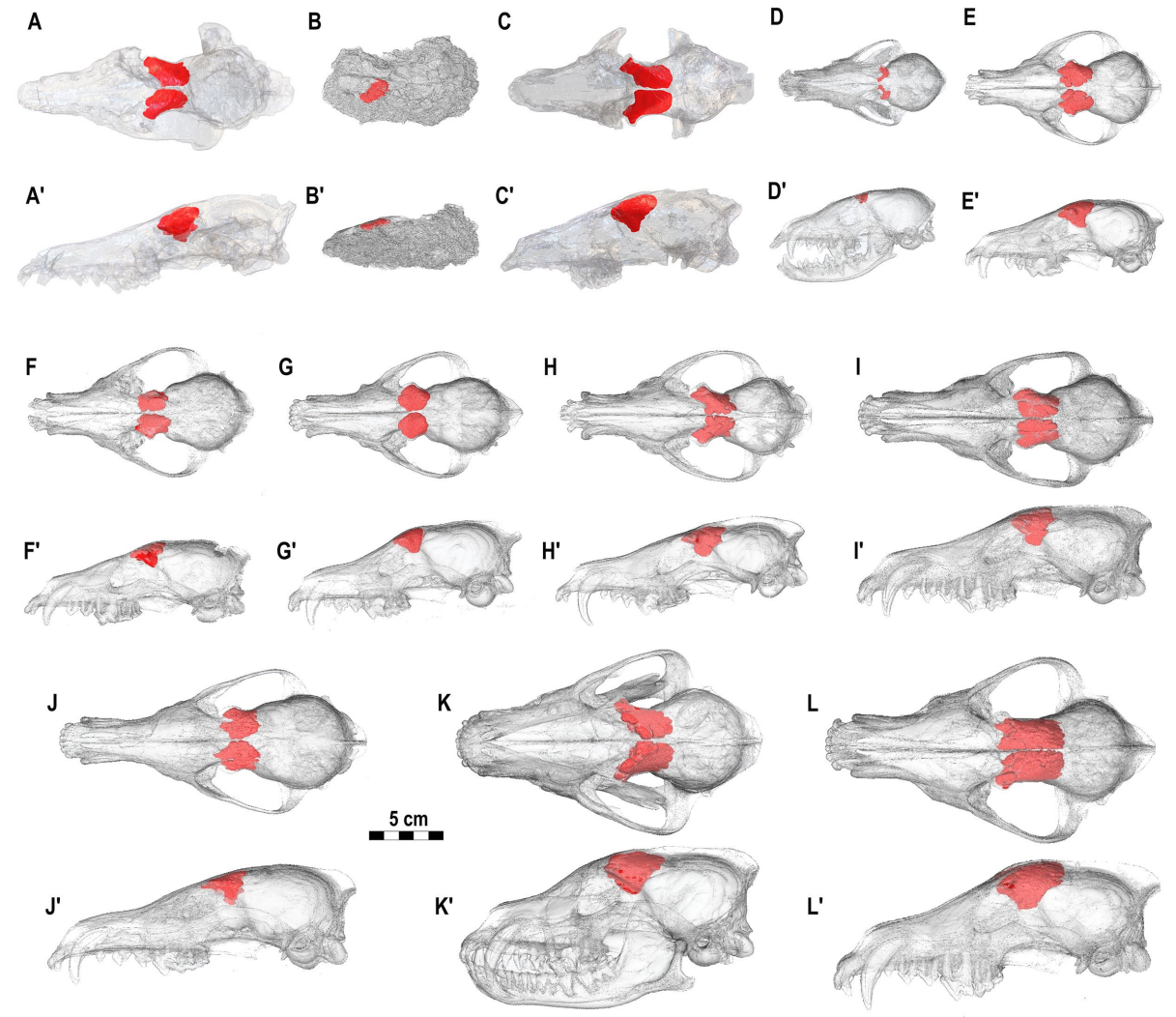

FIGURE 4
Dorsal and left lateral views of the crania of fossil and extant Canidae analyzed here, with the frontal sinuses in their natural position. **(A–A')** NMB Rss.45, *E. adoxus*. **(B–B')** MSF 466, *E. monticinensis*. **(C–C')** F:AM 97057, *E. davisi*. **(D–D')** MZUF-1474, *V. lagopus*. **(E–E')** MZUF-1715, *L. mesomelas*. **(F–F')** MZUF-11878, *C. aureus*. **(G–G')** MZUF-1851, *C. lupaster*. **(H-H')** MZUF-8496, *L. adusta*. **(I–I')** 88-50-290, *C. latrans*. **(J–J')** MZUF-13781, *C. simensis*. **(K–K')** 368.443, *L. pictus*. **(L–L')** MZUF-11874, *C. lupus*.

relationship to the cranium. Figure 5 shows the morphology of the left sinus of a single specimen for each species considered. As it is visible from Figures 4, 5, the frontal sinus is a fairly variable structure, showing a wide range of dimensions and morphologies in the members of the family Canidae. The analysis shows the almost total lack of sinus in *V. lagopus*, which are not well defined nor possess proper lobes, rather many small chambers barely connected to each other. On the contrary, all the other specimens analyzed possessed well-formed sinus, distinguished from one another for their degree of external complexity. Despite these differences all species shared a rounded three-sided outline in lateral view and the presence of at least one rostral lobe. In all the species of *Canis*, two rostral lobes separated by the rostral incision are visible, despite their different degree of development in the various species. *Canis aureus* and *C. lupaster* show very similar frontal sinuses with a shallow rostral incision and a small rostromedial and rostrolateral lobes, while *C. latrans* and *L. mesomelas*, despite still having two fairly small rostral lobes, show a deeper rostral incision (which in the case of *L. mesomelas* is also wider). The postorbital lobe in *C. aureus*, *C. lupaster* and *L. mesomelas* is reduced and barely diversified on the lateral side of the rostrolateral lobe. It also has comparable position in rostrocaudal length of the sinus. The similarity between *L. mesomelas* and *C. aureus* and *C. lupaster* also extends in lateral view: a three-sided outline, with no or modestly developed ventrolateral prominence. *Canis latrans* has a deeper and more developed sinus, in both dorsal and lateral views. *Canis simensis* has a deep, wide, and rounded rostral incision, with two well-formed rostral lobes, especially the rostrolateral one. In general terms, the sinus of the Ethiopian wolf is characterized by a relatively poor rostrocaudal elongation but a proportionally dorsoventrally deep extension. Indeed, in lateral view the sinus shows an angulated and

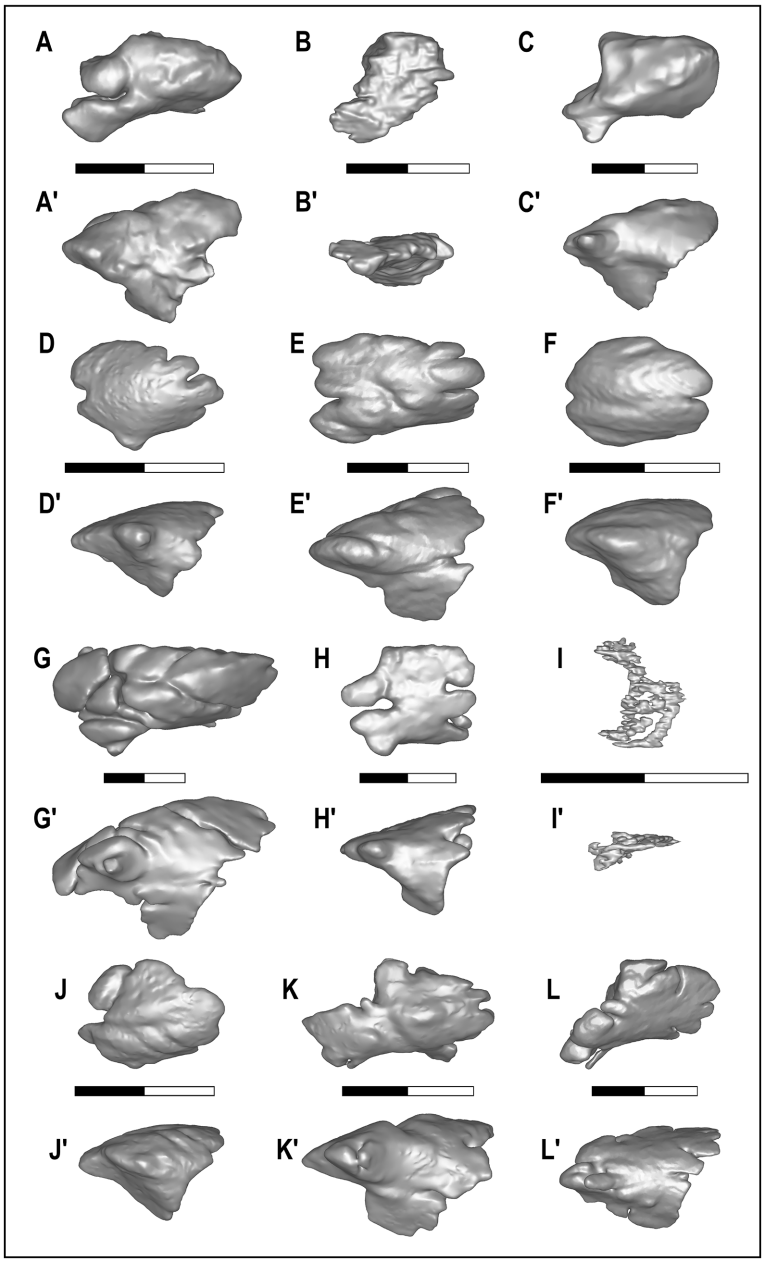

FIGURE 5
Dorsal and lateral views of the left frontal sinus of the examined species. Each model has been reported to same width (and true scale, i.e., 2cm, is reported per each specimen between dorsal and lateral view). **(A–A')** NMB Rss.45, *E. adoxus*. **(B–B')** MSF 466, *E. monticinensis*. **(C–C')** F:AM 97057, *E. davisi*. **(D–D′)** MZUF-11880, *C. aureus*. **(E–E')** 88-50-290, *C. latrans*. **(F–F')** MZUF-2714, *C. lupaster*. **(G–G')** MZUF-2032, *C. lupus*. **(H–H′)** MZUF-13781, *C. simensis*. **(I–I′)** MZUF-1474, *V. lagopus*. **(J–J')** MZUF-3293, *L. mesomelas*. **(K–K′)** MZUF-8496, *L. adusta*. **(L–L')** 368.443, *L. pictus*.

wide ventral lobe. Moreover, it displays a series of caudal incisions which denote multiple caudal lobes. *Canis lupus* possesses the most complex sinus in the genus *Canis*, rivaled only by that of *L. pictus*. In addition to a deep rostral incision, *C. lupus* shows two well-developed and domed rostral lobes and a dorsal sulcus that branches medially and laterally, shaping different prominences. The African hunting dog, *L. pictus*, have a complex and lobose sinus, marked by the developed rostrolateral lobe and a reduced rostromedial one. In this species, the postorbital lobe is rostrally advanced and further pneumatized in two separated lobules. The degree of complexity and of additional prominences of the dorsal surface is similar to that of the wolf. Caudally, the sinus of *L. pictus* is rounded and subdivided into different smaller lobules by evident incisions, similarly but more than in *C. lupus*. In *L. adusta*, the sinus is particularly proportionally elongated rostrocaudally and marked by the absence of the rostromedial lobe. Furthermore, it possesses an enlarged rostrolateral lobe. Despite the breadth of this part, the postorbital lobe is not so expanded, yet invading the zygomatic process of the frontal. The postorbital lobe is parted in two lobules in the considered specimen. Despite the generic attribution, the sinuses of *L. adusta* and

L. mesomelas differ greatly from one another. This is evident in the dorsal shape of the sinuses (slender in *L. adusta*, in dorsal view, and characterized by prominences visible, in lateral view), the morphology of the rostral region and in the development of the caudal lobe and of the ventrocaudal promincence of *L. adusta* (the latter almost in as proper lobe). The morphology of the sinus of *E. davisi* and *E. monticinensis* resembles that of *L. adusta* for the absence of a rostromedial lobe and a developed rostolateral one. Nevertheless, the sinus of *E. monticinensis* is rostrocaudally shorter compared to the one of *L. adusta*. The reduction in rostrocaudal length is similar to *C. aureus*, *C. lupaster*, and *L. mesomelas*. Nevertheless, the taphonomic deformation of the cranium (thus of the sinus) hinders proper comparison with the other extant canids. *Eucyon davisi* instead shows a proportionally reduced rostrolateral lobe when compared to the large and inflated one of *L. adusta*. Furthermore, the sinus of the fossil species is more inflated with almost no subdivisions, whereas *L. adusta* shows numerous lobules individualized by sulci and incisions. Despite these differences the sinus of *L. adusta* is closest in terms of general resemblance to that of *E. davisi*. The sinus of *E. adoxus* differs from that of medium-sized canids (*C. aureus*, *C. lupaster*, *C. latrans*, *C. simensis*, and *L. mesomelas*) for its rostrocaudal elongated and pointed shape, in dorsal view. In this regard, it resembles *C. lupus*, though proportionally smaller. Even in lateral view, *E. adoxus* has a proportionally deep sinus, unlike previous taxa. The dorsal surface shows some prominences identified by a branched sulcus resembling those of *C. latrans* and, to minor extent, *C. lupus*. The presence of a bulging and inflated rostromedial sulcus marks a sharp difference with *L. adusta*.

Another feature used to describe the morphology and development of these paranasal cavities is their caudal extension, in particular relative to the frontoparietal suture. As visible in Figure 4, only in *C. lupus* and *L. pictus* the frontal sinus reaches the frontoparietal suture, whereas in the other species, despite their difference, it never extends further caudally. Other species that have well-developed frontal sinuses with a considerable caudal extension, i.e., close to the frontoparietal suture, are *C. latrans*, *C. simensis*, and *L. adusta*. If the cranium is observed in lateral view (Figure 4), it is relevant to note the relationship between the frontal sinus and the endocranium. The frontal sinus in *V. lagopus* is evidently reduced. In *C. lupus* the frontal sinus covers a good portion of the cranial cavity, whereas in the other species it covers different portions of the braincase. In *C. aureus* the overlap between the frontal sinus and the brain is the smallest (Figure 4). The second is *C. lupaster*, and then *C. simensis* and *C. latrans* which have similar parts of the braincase covered by the frontal sinus. *Lycaon pictus* has a large portion of the braincase topped by the frontal sinus even if the overlapping region is not as large as in *C. lupus*. In *Lupulella* spp., *L. adusta* seems to possess a longer region of the braincase covered by the frontal sinus compared to *L. mesomelas*. As mentioned above, in the fossil species the sinus expands caudally into a modest portion of the endocranial cavity. This extension is comparable in both *E. adoxus* and *E. davisi*. The preservation of *E. monticinensis* specimen (MSF 466) does not allow any comparison.

As far as the morphometric analyses are concerned, the study considered in particular the relationship between different parameters extrapolated by the tridimensional renderings of the frontal sinus (e.g., sinus volume, maximum rostrocaudal length of the sinus) and characteristics of the considered specimens/species (e.g., total length of the cranium, body mass) (Table 2). The results are reported in Table 3 and Figures 6, 7. The sinus of *E. monticinensis* was not considered because it was too deformed for this kind of analysis.

The bivariate regressions for the considered morphometric variables show that they are highly correlated with one another and with the body mass (Figures 6, 7; Table 3). Both ln LmaxS and ln Vol show a strong correlation with ln BM, which explains a similarly large amount of the variance of the two variables (*ca.* 70–75%) and follows a negative allometry relationship (i.e., the body mass grows slower than either volume or the maximum sinus length) (Figures 6A,B). The correlation between ln LmaxS and ln Vol with ln TL is similarly strong, explaining approximately 70% of total variance, yet shows a positive allometry relationships (i.e., the skull length increases faster than both volume and maximum sinus length) (Figures 6C,D). In all plots of Figure 6, *V. lagopus* and *C. lupus* lie at the two extremes of variability, as the former has an extremely reduced sinus, whereas the latter has the largest and most developed sinus of all the considered species. Between these two extremes lie all the other extant species. *Eucyon adoxus* is located close to the variability of *C. simensis*, for its similar values of ln Vol and ln LmaxS, and to the lower ranges of Groups 1 hypercarnivores. *Eucyon davisi* lies a bit apart from the ecomorphological groups. The comparable values of ln LmaxS and ln TL, *E. davisi* is often close to *L. adusta* (as in Figures 6A,C,D). Considering the relationship between ln LmaxS and ln Vol (Figure 7) we have seen an interesting pattern of distribution. Group-hunters canids (Group 1 of Van Valkenburgh and Koepfli, 1993) are separated from the other canids, especially mesocarnivores (Group 3) and small-prey hypercarnivores (Group 2). This is highlighted by the regression lines with different R^2 plotted in the graph (Figure 7; Table 3). The distinction in the lines suggests the presence of an allometric grade shift between group-hunter taxa and the rest of Canidae. This is further confirmed by the ANCOVA results, showing the homogeneity of the allometric slopes ($F = 0.005$, $p = 0.947$) and the presence of significant differences between the intercepts ($F = 136.03$, $p = <0.001$) of the two groups. Hence, group hunters appear to possess a more voluminous sinus for a similar sinus length when compared to non-group hunter canid taxa. Apparently, *L. adusta* lies together with the large-prey hypercarnivores, unlike *E. davisi* or *E. adoxus*, which clustered close, almost overlapped, to *C. simensis*.

3.3. Diffeomorphic analyses

The principal component analysis (PCA) performed on the deformation fields obtained from the DSM analyses performed on the left sinus (Figure 8; Table 3; see Supplementary Material) allows discerning the four different ecological groups included in the study, particularly when the first three principal components (PCs; 46.2% of total variance) are considered at the same time. The bivariate regressions between the PCs and log-transformed BM identify the presence of a significant allometric relationship only for PC2 (Table 3), where the body mass explains half ($R^2 = 0.429$, $p < 0.001$) of its total variance, thus suggesting that BM differences play a limited role in explaining the separation observed between the analyzed taxa. The PC1 accounts for the 20.7% of the variability. Along this axis the groups fail to separate properly, with the majority of the specimens located on the positive side of the axis

TABLE 2 Results of the measurements of the specimens examined.

Species	Cat. Num.	Vol (mm^3)	LmaxS (mm)	TL (mm)	BM (kg)
Eucyon adoxus	NMB Rss.45	2692.9	28.8	182	15.5
Eucyon davisi	F:AM 97057	3014.6	30.6	167.3	11.4
Eucyon monticinensis	MSF 466	985.3*	22.1*	-	12.0[+]
Canis aureus	MZUF-11880	1640.2	24.1	154.2	7.4
	MZUF-11878	1517.8	20.3	151.5	9.2
Canis latrans	88-50-250	3469.3	29.5	197.0	19.6
Canis lupaster	MZUF-1851	1683.4	21.6	156.4	9.6
	MZUF-2140	675.2	15.5	156.3	8.7
	MZUF-2110	712.8	18.4	150.5	8.5
	MZUF-2714	1549.1	20.4	146.5	8.5
Canis lupus	MZUF-2032	11406.5	50.7	220.1	26.0
	MZUF-11874	8772.2	46.5	223.2	26.5
	MZUF-16534	9342.2	44.8	231.5	29.2
	DST-N01	4437.5	39.6	212.6	22.3
Canis simensis	m-81.001	2579.7	28.4	208.4	22.3
	CE818	1789.9	24.3	187.2	16.3
	MZUF-13781	2935.8	28.8	203.4	21.7
Lupulella adusta	MZUF-8496	1920.9	31.4	166.5	13.2
Lupulella. mesomelas	MZUF-1843	1000.1	19.3	-	-
	MZUF-1898	1755.5	24.0	150.1	9.4
	MZUF-1128	942.2	19.7	153.6	9.8
	MZUF-1715	2382.4	26.8	147.1	-
	MZUF-3293	1293.6	22.9	132.3	6.5
Lycaon pictus	368.443	5913.1	44.1	204.0	21.4
	MZUF-1127	3323.3	36.0	192.9	20.0
Vulpes lagopus	MZUF-1474	29.5	9.5	113.1	4.4

*these measures must be taken with caution; [+]estimation taken from Bartolini-Lucenti and Rook (2021), based on the regression formula by Van Valkenburgh (1990) based on length of the lower carnassial.

TABLE 3 Results of ordinary least-squares (OLS) regressions between natural log-transformed metric variables, natural log-transformed body mass, principal components (PCs), and canonical variates (CVs) used to assess the correlation between the used variables.

	R^2	*p*	Slope	SE	95% CI		Intercept	SE	95% CI	
Canidae ($n = 25$)										
ln LmaxS vs. ln Vol	**0.887**	**<0.001**	**0.936**	**0.071**	**0.788**	**1.084**	**0.904**	**0.181**	**0.527**	**1.281**
ln Vol vs. ln BM	**0.699**	**<0.001**	**0.638**	**0.088**	**0.454**	**0.821**	**0.883**	**0.233**	**0.398**	**1.368**
ln LmaxS vs. ln BM	**0.738**	**<0.001**	**0.652**	**0.082**	**0.481**	**0.823**	**1.6**	**0.217**	**1.154**	**2.056**
ln Vol vs. ln TL	**0.695**	**<0.001**	**1.767**	**0.242**	**1.266**	**2.269**	**−6.564**	**1.247**	**−9.149**	**−3.979**
ln LmaxS vs. ln TL	**0.718**	**<0.001**	**1.788**	**0.232**	**1.307**	**2.268**	**−5.912**	**1.195**	**−8.390**	**−3.434**
PC1 vs. ln BM	0.122	0.062	−0.402	0.204	−0.827	0.022	1.07	0.546	−0.069	2.209
PC2 vs. ln BM	**0.429**	**<0.001**	**0.554**	**0.135**	**0.272**	**0.837**	**−1.426**	**0.363**	**−2.183**	**−0.668**
PC3 vs. ln BM	0.016	0.567	0.096	0.165	−0.249	0.441	−0.264	0.443	−1.188	0.661
CV1 vs. ln BM	**0.317**	**0.004**	**−4.742**	**1.448**	**−7.763**	**−1.722**	**11.853**	**3.883**	**3.753**	**19.952**
CV2 vs. ln BM	**0.281**	**0.007**	**−2.409**	**0.793**	**−4.063**	**−0.754**	**6.492**	**2.128**	**2.054**	**10.931**
Group hunters ($n = 6$)										
ln LmaxS vs. ln Vol	**0.091**	**0.002**	**0.731**	**0.104**	**0.443**	**1.0187**	**1.628**	**0.304**	**0.783**	**2.472**
Non-group hunters ($n = 19$)										
ln LmaxS vs. ln Vol	**0.86**	**<0.001**	**0.75**	**0.075**	**0.59**	**0.91**	**1.304**	**0.181**	**0.919**	**1.689**

Significant correlations are in bold.

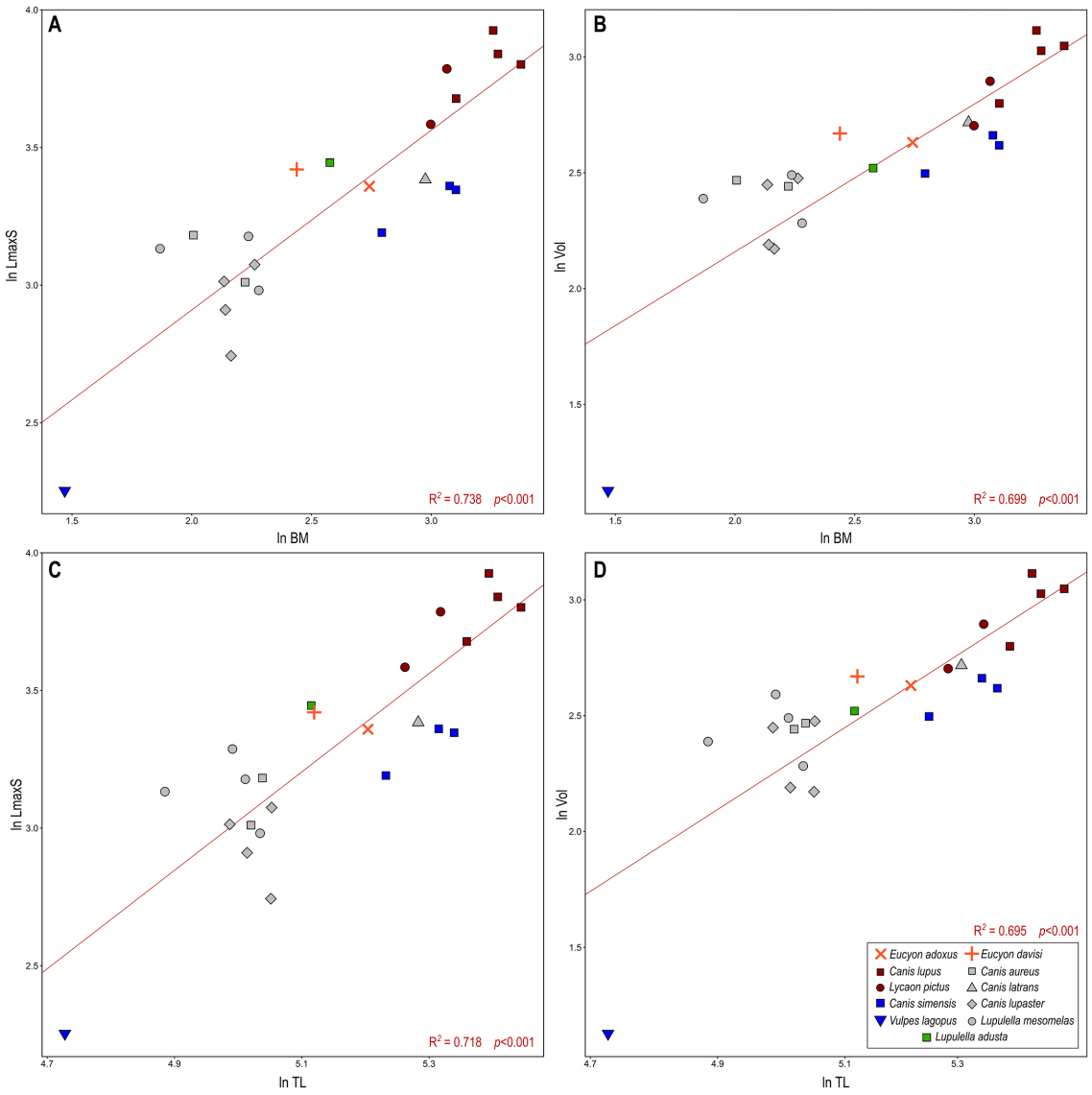

FIGURE 6
Bivariate regressions between **(A)** the natural log-transformed body mass (ln BM) vs. the log-transformed maximum rostrocaudal length of sinus (ln LmaxS). **(B)** The log-transformed body mass (ln BM) vs. the log-transformed of cubic root of volume of the sinus (ln Vol). **(C)** The natural log-transformed total length of the cranium (ln TL) vs. the log-transformed maximum rostrocaudal length of sinus (ln LmaxS). **(D)** the natural log-transformed total length of the cranium (ln TL) vs. the log-transformed of cubic root of volume of the sinus (ln Vol). Lines represent OLS (ordinary least squares regressions) best-fit lines for the whole canid sample. There is a significant correlation between all the variables (see Table 3 for further details).

and very few on negative values. *Canis lupus* and *L. pictus* (Group 1) show a wide-range variability along PC1. Apart from one specimen of *L. mesomelas*, both *Canis simensis* (Group 2) and canids of Group 3 placed in the positive side of PC1. This position corresponds to proportionally inflated (especially laterolaterally and dorsoventrally) but rostrocaudally shortened sinuses – see Figure 8C. This pattern is confirmed by their morphology (see Figure 5). *Eucyon adoxus* lies close to *C. simensis*, with a slightly low negative value of PC1. *Eucyon davisi* falls within the variability of Groups 1 and 3. PC2 accounts for 14.7% of the morphological variability. Along this axis the ecological groups are almost separated, with Groups 2 placed on the positive side of PC2, whereas the majority of Group 3 and the specimen of *L. adusta* have the negative values of the axis. Most of the specimens of Group 1 canids have high positive values of PC2. The fossil species have small positive values of PC2. The PC3 accounts for the 10.8% of the variability. Along this axis the groups are almost all clustered together toward positive values (between −0.25 and 0.5). *Eucyon* spp. lie within this cluster of extant species.

The canonical variate analysis (CVA; Figure 9) performed on the first four principal components achieves good classification results after cross-validation, with 95.2% of correctly classified individuals. A visual inspection of the bivariate plot of CV1 and CV2 confirms this result and shows a very good separation between the *a priori* identified ecological groups, with no overlap among them (Figure 9) along CV1 (80.5% of total variance). Notably, CV1 and CV2 show a strong and

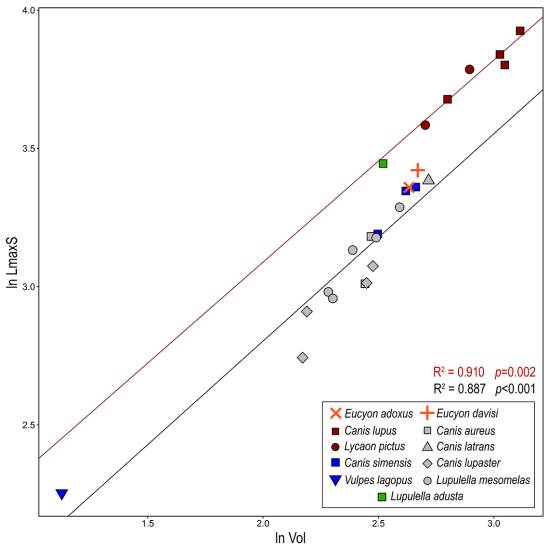

FIGURE 7
Bivariate regressions between the natural log-transformed of cubic root of volume of the sinus (ln Vol) and log-transformed maximum rostrocaudal length of sinus (ln LmaxS). Lines represent OLS (ordinary least squares regressions) best-fit lines for the whole canid sample (black) and hypercarnivorous group-hunting canids (red). There is a significant correlation between volume and the length of the sinus (see Table 3 for further details).

significant correlation with the body mass (Table 3), which explains less than half (CV1: $R^2 = 0.317$, $p = 0.004$; CV2: $R^2 = 0.281$, $p = 0.007$) of its variance. Thus implying that BM plays a role in the shape differences captured by these axes, while not being the main driver of shape variation. This is also partially reflected by the distribution of the groups along the CV1, all clearly separated from one another. Specimens of Groups 1, 2 and 3 cluster fairly well and lie at the opposite sides of the axis, respectively in its negative (Group 1) and positive (Groups 2–3) portion. The two extremes are related to completely different shapes of the sinus: the lowest values of the CV1 coincide with rostrocaudally elongated and narrow sinus, with strong rostrolateral lobes; on the contrary, the high values of CV1 correspond to laterolaterally inflated and short sinus, see Figure 9B. In between them lies the single specimen of *L. adusta*. The fossil species are located in the negative side of the axis: *E. adoxus* is enclosed in the variance of Group 1 canids, whereas the *E. davisi* has the lowest value of CV1. On the CV2 (19.5% of variance) the specimens do not separate greatly and most of them are rather comprised between −2 and 2. Only *C. simensis* lies far, with peculiarly negative low values. Along this axis, *E. adoxus* confirms its position close to Group 1 canids. *Eucyon davisi* has very high values, lying far from any group. This corresponds to fairly rostrocaudal short sinuses with developed rostral lobes. The posterior probabilities computed for *E. adoxus*, *E. davisi* and *L. adusta* on the basis of CVA scores classify these taxa as group-hunters, with a posterior probability of 100% for both fossil species and 94% for *L. adusta* (Table 4). In contrast, the typicality probabilities—which do not imply that each specimen must belong to at least one of the groups as posterior probabilities do— show that *L. adusta* and *E. davisi* represent outliers for all the considered ecological groups ($p < 0.05$). In turn, *E. adoxus* matches the variability of group-hunters ($p = 0.30$; Table 4) confirming the result of posterior probabilities.

4. Discussion

4.1. Frontal sinus: phylogenetic signal and ecological relevance

Among carnivorans, the frontal sinus as anatomical structure has been deeply studied in Hyaenidae (Vinuesa et al., 2016) and recently in Ursidae (Pérez-Ramos et al., 2020). Frontal sinus in fossil hyaenids were firstly described by Joeckel (1998), evidencing that bone-cracking forms like *Adcrocuta* possessed very enlarged frontal sinus overlapping the whole brain cavity and other jackal-like, wolf-like and transitional bone-cracker forms with lesser enlarged sinus which only overlap from 70 to 80% of the brain cavity like *Hyaenotherium*, *Palinhyaena* (Qiu et al., 1979) or *Ictitherium* (Joeckel, 1998; see also Vinuesa et al., 2015, 2016; Vinuesa, 2018, for further discussion). Despite the interesting convergent evolution between hyaenas and canids (see Supplementary Material), even in terms of frontal sinus development, that of fossil canids was never studied in detail, except for a few cases. For instance, some scholars hypothesized a posteriorly enlarged frontal sinus in some hypercarnivorous and durophagous American fossil canids like *Borophagus* (Cope, 1892) and *Epicyon* (Leidy, 1858) (see Werdelin, 1989; Tseng and Wang, 2010).

In Caninae, i.e., extant canids, the features of the frontal sinus were described for the first time by Huxley (1880), who used them as one of the main characteristics to differentiate between "Alopecoid" and "Thooid" canids. In his view, the division is justified by the lack of the frontal sinus in the former and their retention in the latter. Some scholars discarded this interpretation relating it to an increasing size (e.g., Matthew, 1924), whereas others maintained the unrelatedness between frontal sinus development and body size (we will discuss this further on). The latter interpretation favored the validity of frontal sinus features for phylogenetic interpretations such as those of Berta (1988) or Tedford et al., (1995, 2009). The studies of the late R.H. Tedford, together with X. Wang and B.E. Taylor, are among the most relevant analyses of the frontal sinus in extant and fossil Caninae. In their papers, the authors studied the absence or presence of the sinus, and its development in terms of expansion toward the postorbital process of the frontal, in lateral sense, and the frontoparietal suture, in caudal sense. Anatomical and paleontological evidence supports the interpretation of a phylogenetic information in the expansion of the frontal sinus: the early forms of Caninae (e.g., *Leptocyon* Matthew, 1918) lack a developed sinus (Tedford et al., 2009), as does most of the extant and fossil representatives of the genus *Vulpes* and *Urocyon* (Baird, 1858). In juxtaposition to this condition, *Canis* spp. have inflated sinuses that always invade the postorbital process and, in some taxa, extends toward the frontoparietal suture. The similarities between *Leptocyon*, *Urocyon* and *Vulpes* in terms of morphological features and the timing of their paleontological record (the genus *Leptocyon* is the oldest of the subfamily Caninae known since the Oligocene, whereas *Vulpes* and *Urocyon* are the oldest of extant canids to appear in the fossil record; Tedford et al., 2009) suggest the primitive nature of the absence/reduction of the frontal sinus in Caninae (confirmed also in Canidae by other observations, e.g., Wang, 1994; Wang et al., 1999). And at the same time the development in *Canis* apparently marks the derivate state of these taxa. This observation is corroborated by empirical evidence and was often used also with a systematic purpose. Tedford and Qiu (1996) included the lateral inflation of the sinus into the

10.3389/fevo.2023.1173341

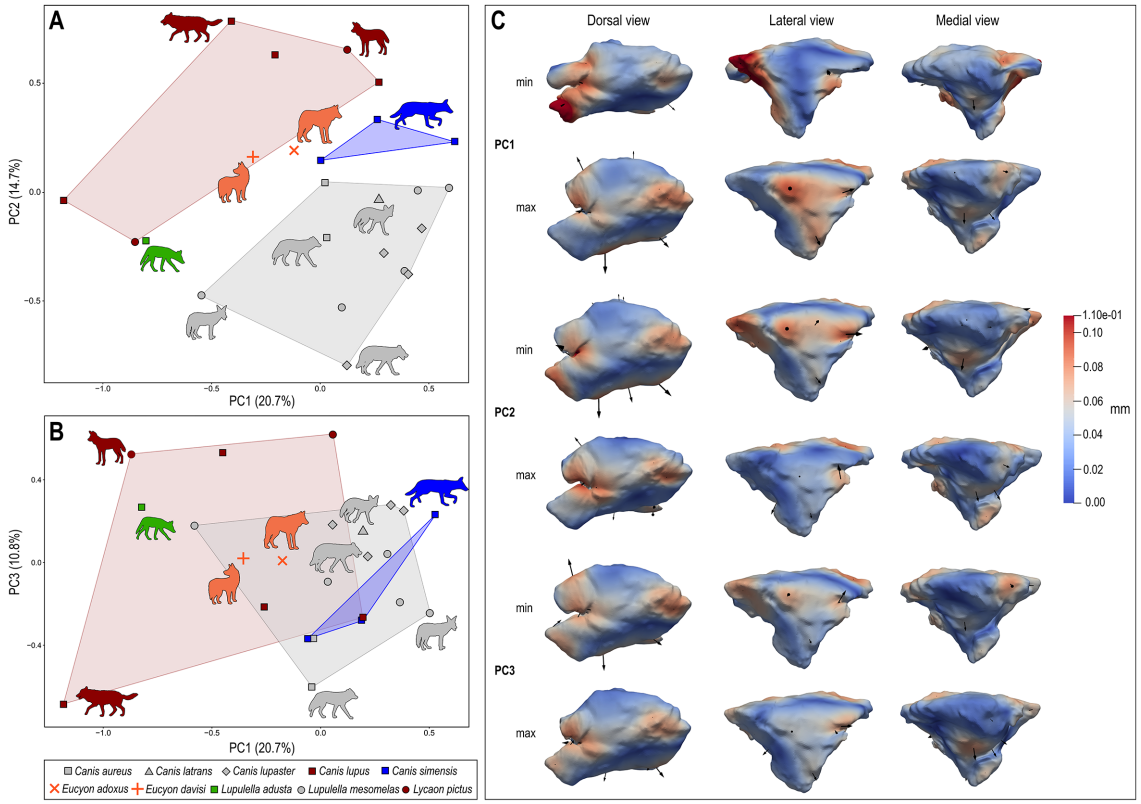

FIGURE 8
Bivariate scatterplots of PCA results performed on the deformation fields obtained from DSM analysis of sinus shape (variance for each component included within parentheses): **(A)** PC2 vs. PC1; **(B)** PC3 vs. PC1. **(C)** Maximum (below) and minimum (above) extreme conformations of shape variation are shown in dorsal (left), lateral (middle), and medial (right) views for each PC: PC1, PC2, and PC3. Cumulative deformations from mean shape are mapped on the surface by means of a pseudocolor scale ranging from dark blue (no displacement) to dark red (0.11mm). Black arrows correspond to the vectors identifying the direction and amount of displacement. Symbols and convex hulls are colored group-wise as follows: dark red – hypercarnivorous group hunters; grey – mesocarnivores; blue – hypercarnivores on small prey; green – hypocarnivores.

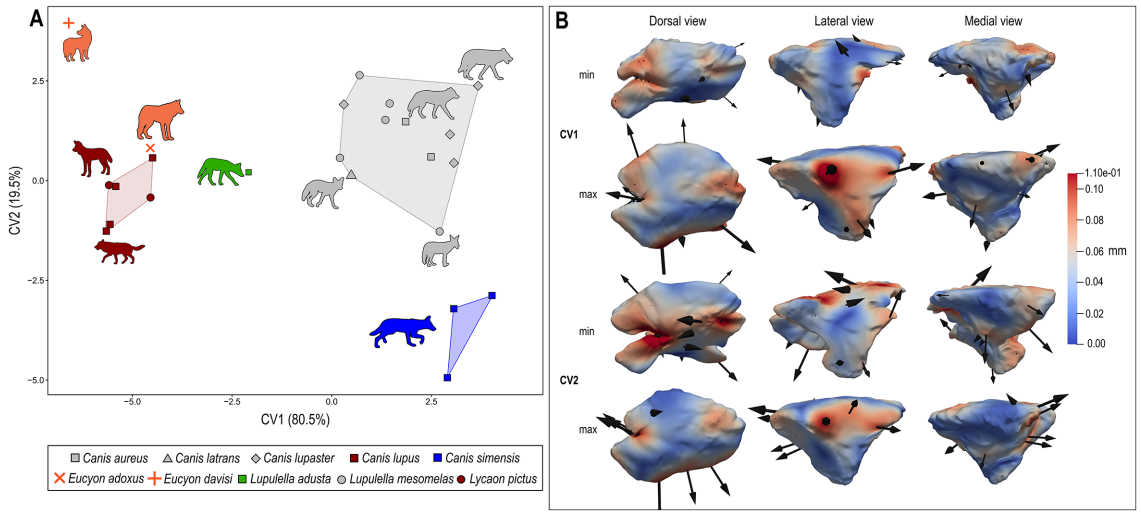

FIGURE 9
(A) Bivariate scatterplots of CVA results performed on the deformation fields obtained from DSM analysis of sinus shape (variance for each canonical variate included within parentheses). **(B)** Maximum (below) and minimum (above) extreme conformations of shape variation are shown in dorsal (left), lateral (middle), and medial (right) views for each CV: CV1 and CV2. Cumulative deformations from mean shape are mapped on the surface by means of a pseudocolor scale ranging from dark blue (no displacement) to dark red (0.11mm). Black arrows correspond to the vectors identifying the direction and amount of displacement. Symbols and convex hulls are colored group-wise as follows: dark red – hypercarnivorous group hunters; grey – mesocarnivores; blue – hypercarnivores on small prey; green – hypocarnivores.

TABLE 4 Posterior and typicality probabilities computed for *E. adoxus*, *E. davisi*, and *L. adusta* based on canonical variate analysis (CVA) scores obtained using hunting strategy as a grouping factor.

	Group hunters	Hypercarnivores	Mesocarnivores
Posterior probabilities			
E. adoxus NMB Rss.45	100%	0%	0%
E. davisi F:AM 97057	100%	0%	0%
L. adusta MZUF-8496	94%	0%	6%
Typicality probabilities			
E. adoxus NMB Rss.45	**0.38**	<0.001	<0.001
E. davisi F:AM 97057	<0.001	<0.001	<0.001
L. adusta MZUF-8496	0.01	<0.001	<0.001

Note that while posterior probabilities represent the likelihood of belonging to a group (expressed as a percentage), typicality probabilities are given as *p*-values for the null hypothesis of group membership so that for $p < 0.05$, the specimen can be considered an outlier for a given group. Highest posterior probabilities and significant typicality probabilities are in bold.

postorbital process as one of the diagnostic features of the genus *Eucyon*, a synapomorphy shared with *Canis*. Sotnikova (2006) described a peculiar Canini from the Pliocene of Mongolia as *Nurocyon chonokhariensis* thanks to a combination of primitive and derived features, among which sharing a large frontal sinus that invades the postorbital process with *Canis* and *Eucyon*.

Nevertheless, the information from the structure and development of the frontal sinus has also led to some phylogenetic reconstructions that contrast with molecular evidence. One of the most striking probably is relationship between the crab-eating fox (*Cerdocyon* Smith, 1839) and the raccoon dog (*Nyctereutes*): some morphological analyses (Tedford et al., 2009) include the two taxa within the Cerdocyonina (subtribe erected by Tedford et al., 2009 to include the clade of South American Caninae) whereas the molecular and total-evidence phylogenies show the distance between them (see also Figure 1). While the position of *Cerdocyon* is confirmed, *Nyctereutes* is deeply rooted within the tribe Vulpini, well separated from Canini (among others, Lindblad-Toh et al., 2005; Wayne and Ostrander, 2007; Chen and Zhang, 2012; Zrzavý et al., 2018; Figure 1). This incongruence can be explained by observing the numerous similarities that the crab-eating fox and the raccoon dog show in their cranial and dentognathic features. Among these comparable features there are the prominent subangular lobe, the expanded angular process, the reduced canines, and the development of the frontal sinus, clearly visible from a direct study of cranial specimens (Tedford et al., 1995). These characteristics are linked to diet and ecological preferences and thus most probably they represent convergent features evolved in two distantly related groups, in different context (Eurasia for *Nyctereutes* and South America for *Cerdocyon*) (Bartolini-Lucenti et al., 2018). Indeed, the development of sinuses in *Nyctereutes* has been related by some authors to the possibility of producing relatively large bite forces while feeding (Curtis, 2014; Curtis and Van Valkenburgh, 2014), just like in larger canids (Slater et al., 2009; Tseng and Wang, 2010). Similar ecological interpretation, rather than phylogenetic one, was applied to the Late Miocene taxon *Eucyon ferox* (Miller and Carranza-Castañeda, 1998). Once considered the first member of the genus *Canis*, also due to the development of its frontal sinus, a recent reassessment of its general features suggests a more plausible interpretation of the taxon to the genus *Eucyon* and with a hypercarnivorous diet (Bartolini-Lucenti and Rook, 2021). As in the case of *Nyctereutes*, the development of the sinus of *E. ferox* is thus plausibly related to its diet.

4.2. Frontal sinus and inferred diet preferences

Despite the variability displayed by this structure, the comparison of different morphologies of the frontal sinus possessed by the different canids has shown some patterns (Figure 5). Most of the features discussed above seem to correspond to an ecological affinity rather than a phylogenetic relationship between species with similar sinus morphologies. Indeed, in some cases, phylogenetically related taxa differ more than with distantly related ones. For instance, the species identified as mesocarnivorous (*C. aureus*, *C. latrans*, *C. lupaster* and *L. mesomelas*; n.b., all members of Group 3) have comparable general shapes of the sinuses. They show, e.g., shallower rostral incisions and modest and simple rostrolateral lobes, less developed compared to the hypercarnivorous ones, like *C. lupus* (Group 1) and *C. simensis* (Group 2). Moreover, mesocarnivorous species share fairly smooth dorsal surface of the sinus, without marked sulci on it. The only exception to this smooth pattern is *C. latrans*, which shows a particularly evident caudal prominence, identified by a transverse dorsal sulcus (Figure 5). As far as hypercarnivorous species are concerned, it should be noted that Groups 1 and 2 show a great difference between them: the former has simpler lobes in the rostral region whereas the latter has more developed and more complex rostral lobes. Furthermore, the sinus of *C. simensis* has low prominences on its dorsal side, although some sulci are still visible on its surface, and, in general terms, are deeper than those of mesocarnivorous canids. On the contrary, the sinus of *C. lupus* is considerably more complex and marked by deep sulci and evident prominences (Figure 5). A great complexity and pneumatization is evident also in *L. pictus*. *Lupulella adusta*, here represented by a single specimen, has its own peculiarities. Unlike the mesocarnivorous species, the sinus is developed, elongated rostrocaudally and possesses relatively high prominences on its dorsal surface. The grouping of taxa according to ecological affinity is testified also by the morphometric analyses here carried out (Figures 6–9). Independently from the methodology and the application (i.e., log-transformed measures or 3D meshes), the results coherently point out two distinct groups, separated from one another. All this evidence fits with the inferences of other scholars (e.g., Curtis and Van Valkenburgh, 2014) on the degree of pneumatization and the development of the frontal sinus according to feeding ecology. The grade shift between group hunters (Group 1) and the others, despite their diet (namely Group 2–3) add

further support to this interpretation (Figure 7). Interestingly, the position of *L. adusta* matches the hypothesis: larger stresses during feeding (whether from food items or prey hunting) seem to result in comparably larger and convoluted sinuses in group hunters and hypocarnivorous canids. If such inference can be easily drawn from Group 1 species, in the case of Group 4 ones (though here represented by a single specimen), at the very least, the results corroborate the observation by Curtis and Van Valkenburgh (2014) regarding *N. procyonoides* (another typical hypocarnivorous, i.e., Group 4, taxon, following Van Valkenburgh and Koepfli, 1993).

Therefore, our analyses confirm how relevant frontal sinus is as an anatomical structure and yet the numerous parameters that influence its development. Surely, like Matthew (1924) hypothesized, body mass has an influence on the development of the sinus. Nevertheless, the influence of phylogeny pointed out by several scholars (e.g., Berta, 1988; Tedford et al., 2009; see above) is undeniable. Generally, members of the tribe Vulpini do not have frontal sinus, whereas, on the contrary, Canini always do possess the sinus, with different development (Figures 4, 5). When comparing the morphology of the sinus within Canini, some phylogenetically controlled features seem to be present (e.g., an expanded rostromedial lobe in *Canis* s.s. unlike *Lupulella*). Nevertheless, other smaller scale differences or peculiar similarities between the species here considered cannot be easily explained with phylogeny. The third parameter with a relevant role in shaping the frontal sinus of canids is their ecology, in terms of dietary habits. Indeed, this structure is linked to a complex and interrelated set of characteristics which must be simultaneously taken into consideration when studying fossil species. Despite the deformation that hinders morphometric analyses, the sinus of *E. monticinensis* is modestly developed and characterized by a similarity with the genus *Lupulella*, rather than *Canis*. This similarity is shared also by *E. davisi*. In both fossil taxa, the developed rostrolateral lobe marks this similarity, especially with *L. adusta*. Despite the mild deformations, the similarity of the sinus of *E. monticinensis* with the species of the African *Lupulella* is interesting for its timing. *Eucyon monticinensis* represents one of the oldest undisputed records of Canidae in western Eurasia (age of the type locality: *ca* 5.6–5.3 Ma; Rook, 1992; Bartolini-Lucenti et al., 2022; Figure 1), part of the '*Eucyon* event' of the Late Miocene (Sotnikova and Rook, 2010). The time of divergence of the genus *Lupulella* from the *Canis*-clade following recent molecular analyses (e.g., Perri et al., 2021) is estimated around 5.1 Ma. There are Late Miocene records of *Eucyon* in Africa (e.g., *E. intrepidus* from Kenya), which nevertheless were recently disputed by some authors for the scanty nature and the inconsistency of their features (see Werdelin et al., 2015 for a deeper discussion on the issue). Taxa typical of '*Eucyon* event', e.g., *E. monticinensis* and *E. davisi* from Asia (Sotnikova and Rook, 2010), could be at the base of the radiation of this jackal-like canids in Eurasia but also in Africa. *Lupulella* might be the extant descendant of such dispersal and radiation. The interpretation does not contrast with present phylogenetic hypotheses (e.g., Zrzavý et al., 2018) and finds support in the patterns of morphological and morphometric affinities obtained here. Regarding *E. davisi*, linear morphometric parameters were not conclusive in classifying the diet of this fossil taxa with any of extant dietary groups, if not for a similarity with Group 3 species (Bartolini-Lucenti and Rook, 2021). Dentognathic features do not hint at any peculiar dietary specialization to hypo- or hypercarnivory (Rook, 2009). Our results show certain degree of peculiarity of *E. davisi* compared to other species, which lies close to *L. adusta* in the linear models (Figure 6) but does not follow the allometric grade shift between natural log-transformed volume and maximum length (Figure 7) and clearly differs from all other groups when total shape is considered (Figures 8, 9).

Different is the case of *E. adoxus*. The development of the rostromedial lobe, or the prominent convoluted dorsal morphology does not support a similarity to mesocarnivorous species (Group 3). This interpretation can be disregarded also considering the results of the morphometric analyses (Figures 6–9). It also differs from the proportionally wider and shallower sinus of *C. simensis*. Morphologically and morphometrically, our results suggest that *E. adoxus* was subject to a relevant amount of stress, comparable, proportionally, to that experienced by Group 1 canids. Such a similarity contrasts with its cranial and dentognathic features, which do not support an ascription to this ecomorphogroup (see also Bartolini-Lucenti and Rook, 2021). It could be argued that even the single specimen of *L. adusta* falls close to hypercarnivorous group-hunters in some analyses (Figures 7, 8; Table 4) and yet the morphological features of this canid are clearly hypocarnivorous. Even in this case, an ascription of *E. adoxus* to hypocarnivorous group can be easily excluded for its dentognathic features. The elongated cranium, the diastemata between premolars, with their pointy cusps, and sharp molars are more definitely close to those of *C. simensis*. Nevertheless, as reminded above, the distinction in terms of frontal sinus development between *E. adoxus* and *C. simensis* is significant. Studying the frontal sinus of Group 2 species is difficult as three out of four species ascribed at this ecomorphogroup are of the genus *Vulpes*, with virtually no sinus [*V. lagopus*, see the 'protosinus' in Figure 5; *Vulpes macrotis* (Merriam, 1888) and *Vulpes corsac* (Linnaeus, 1768)]. The only representant that possesses a sinus is *C. simensis*, and even in this species it is not particularly expanded nor so convoluted (see Figure 5). Almost resembling the condition of Group 3 canids (e.g., *C. aureus* or *C. lupaster*). The hypercarnivorous diet of this canid, based primarily on rodents like the big-headed African mole-rat (*Tachyoryctes macrocephalus* Rüppell, 1842) (Kingdon, 1989), does not imply elevated stresses for their masticatory apparatus. This explains the morphology and modest development of *C. simensis* sinus, despite the degree of carnivory especially in comparison with mesocarnivorous (Group 3). Much evidence supports this: for instance, Van Valkenburgh and Koepfli (1993) showed that, indeed, mesocarnivorous species have more robust mandibles compared to Group 2 species. The cranial and dental morphology of *E. adoxus* fit with the interpretation of this taxon as small-prey hypercarnivorous (Group 2). The more convoluted sinus of *E. adoxus* cannot be explained suggesting that it was capable of hunting large prey, like some Group 3 taxa, as neither its linear morphometric parameters (Bartolini-Lucenti and Rook, 2021) nor the tridimensional morphology of the sinus support it. More plausibly the preferred prey of this canid was larger than those of *C. simensis*. Bartolini-Lucenti and Rook (2021) used the least regression equation of Van Valkenburgh et al. (2003) to estimate typical prey size of *E. adoxus*, obtaining a prey weight of 5 kg. This estimation greatly exceeds the average size of the larger typical prey of *C. simensis* (*T. macrocephalus*: ~400–900 g, Yalden, 1985) and it is close to extant leporid lagomorphs like hares (genus *Lepus* Linnaeus, 1758). A connection between elongated cranium and mandible, characterized by diastemata, and a lagomorph-based diet was proposed for other

fossil canids, e.g., *Cynotherium sardous* (Studiati, 1857) from Sardinia (see Lyras et al., 2006; Lyras and Van der Geer, 2006; Madurell-Malapeira et al., 2015). Lagomorphs experienced a moment of great radiation at the beginning of the Pliocene (Lopez-Martinez, 2008) and dispersal events characterizing different regions and bioprovinces of Eurasia (Maridet et al., 2007). Among the large rodents and lagomorphs of the Early-Late Pliocene of western Europe, several taxa were present, e.g., *Castor* (Linnaeus, 1758); *Trogontherium* (von Waldheim, 1809); *Hystrix* (Linnaeus, 1758); *Hypolagus* (Dice, 1917); and *Oryctolagus* (Lilljeborg, 1874) (see Hugueney, 2004; Lopez-Martinez, 2008). Of these, the former three are generally of large size (Hugueney, 2004), despite the presence of a small-sized *Trogontherium minus* (Newton, 1890) that was found in Red Crag (MN15, UK, Fostowicz-Frelik, 2008) and Perrier-Les Etouaries (Hugueney et al., 1989). Although the latter site is younger than type locality of *E. adoxus*, St. Estève (Roussillon Basin; France; Nomade et al., 2014), the former site is one of the few other occurrences of *E. adoxus* in Europe (Rook, 2009). The Pliocene leporine lagomorph *Hypolagus* (extinct) and *Oryctolagus* were surely smaller compared to the larger rodents before mentioned, but still robust forms compared to the extant species, like *Oryctolagus laynensis* (López Martínez, 1977) (see López-Martínez, 1989; Lopez-Martinez, 2008). They were recorded in the late Early and Late Pliocene of western Europe, also in the Roussillon basin (Mein and Aymar, 1984) together with *Trischizolagus* (Radulesco and Samson, 1967) (another leporine lagomorph). *Eucyon davisi* apparently fed on smaller prey, since the estimated prey size is around 2 kg (Bartolini-Lucenti and Rook, 2021). Interestingly even for *E. monticinensis* the estimated prey size is around 5 kg

FIGURE 10
Restoration of the three *Eucyon* species studied here with their fossil crania highlighting the position of the frontal sinuses, in red. Top: *Eucyon davisi* and the cranium F:AM 97057, on the right. Centrum: *Eucyon adoxus* and the specimen NMB Rss.45, on the left. Bottom: *Eucyon monticinensis* with fragmented cranium MSF 466. Artwork by Cecilia Loddi.

(Bartolini-Lucenti and Rook, 2021). Nevertheless, neither the latter two *Eucyon* spp. possess a specialized dentition nor mandibular features allowing us to narrow down a preferred diet. The morphology of their sinuses seems non-conclusive either.

5. Concluding remarks

Despite the known relevance of the frontal sinus for the phylogeny and ecology of Carnivora, no previous work has ever focused specifically on the morphology of this structure in extant and fossil canids nor described it in detail. This study represents the first attempt to characterize the frontal sinus of Canidae, using CT and micro-CT scans to assess its 3D shape via an innovative 3D geometric morphometric method (i.e., diffeomorphic surface matching analysis), which allows the direct comparison between continuous surfaces in a landmark-free fashion.

The results for extant Caninae show a great correspondence between morphology and renowned ecomorphotype (see Van Valkenburgh and Koepfli, 1993) supporting previous interpretations on the direct influence of diet and feeding behavior on the relative development of frontal sinus in the different canid species. Regarding the fossil species, we were able to reconstruct for the first time the whole sinuses of three *Eucyon* spp. (Figure 10) and compare them with the extant species. The deformation of the specimen of *E. monticinensis* from Cava Monticino does not allow a proper study of the sinus. On the contrary, *E. adoxus*, one of the most enigmatic canids of the Pliocene of the western Eurasia, show a sinus with developed prominences testifying to a relevant stress during feeding, proportionally like hypercarnivorous canids, if not even group-hunters. The dentognathic features of *E. adoxus* do not support an interpretation of this early Canini as a hunter of large prey but more of small prey specialist, like *C. simensis*. The resemblance between these two species can also be retraced to the cranial and mandibular characteristics.

The novel combination of morphological, linear and 3D morphometric analyses has allowed the first rigorous characterization of the frontal sinus of fossil canids of the genus *Eucyon* (Figure 10), revealing the importance of such anatomical structure and its deep connection with size, phylogeny, and ecology of the considered species. The methodology and the analyses here carried out for the first time could be useful tools to help characterizing the frontal sinus and investigating the dietary preferences of fossil carnivorans.

Data availability statement

Publicly available datasets were analyzed in this study. This data can be found at: http://dx.doi.org/10.5281/zenodo.7836886.

Author contributions

SF segmented the tomographic data and prepared a preliminary draft of the text with the help of SB-L and LR. SB-L prepared the linear and 3D data and performed statistical analyses. AU carried out the geometric morphometric analysis. SB-L, JM-M, and AU prepared the manuscript with the contribution of SF, LR, and LC. All author revised and approved the final version of the text.

Funding

SB-L is supported by the Tuscany Region funds for young researchers "Giovanisi" (www.giovanisi.it): "POR FSC 2014–2020" funds for "Progetti di alta formazione attraverso l'attivazone di Assegni di Ricerca." LR acknowledges the support of CHANGES Foundation to the University of Florence (Earth Sciences Department), funded by the Italian Ministry of University and Research, PNRR, Missione 4 Componente 2, "Dalla ricerca all'impresa," Investimento 1.3, Project PE_0000020.

Acknowledgments

The authors are thankful to the kindness of the curators who allowed us to scan the specimens in their collections or to access them online: Paolo Agnelli, curator of the Zoological Museum "La Specola" (Museum of Natural History of the University of Florence, Italy); Enzo Bagnaresi and Marco Sami of the Civic Museum of Natural Sciences of Faenza (Italy); Laurel Lamb of the University of Arkansas Museum (Fayetteville, Arkansas, U.S.A.); Neil Duncan, Collections Manager of the American Museum of Natural History (New York, U.S.A.); Jessie Maisano, Department of Geological Sciences, Jackson School of Geosciences, University of Texas at Austin (U.S.A.). They are indebted to the staff of the San Giovanni di Dio Hospital (Florence, Italy), especially to Elisabetta Peruzzi and Giovanni Dedola and all the technicians of Medical Radiology ward ("SOS Radiologia") for granting us access to their CT-scanner and support while processing raw data. We thank greatly Georgios Lyras for kindly providing us the scan of *E. davisi*. They thank Georg Schulz and Bert Müller for access to the CT-scanner at the Biomaterials Science Center of the University of Basel. We thank Cecilia Loddi for the gorgeous restoration of our *Eucyon* species.

Conflict of interest

The authors declare that the research was conducted in the absence of any commercial or financial relationships that could be construed as a potential conflict of interest.

Publisher's note

Supplementary material

The Supplementary material for this article can be found online at: https://www.frontiersin.org/articles/10.3389/fevo.2023.1173341/full#supplementary-material

References

Baird, S.F. (1858). *Mammals: Upon the zoology of the several Pacific railroad routes. Reports, explorations and surveys for railroad route from Mississippi River to Pacific Ocean 8*: xix–xlviii, 1–757. Washington, DC: Tucker.

Balzeau, A., Albessard-Ball, L., Kubicka, A. M., Filippo, A., Beaudet, A., Santos, E., et al. (2022). Frontal sinuses and human evolution. *Sci. Adv.* 8:eabp9767. doi: 10.1126/sciadv.abp9767

Bartolini-Lucenti, S., Bukhsianidze, M., Martínez-Navarro, B., and Lordkipanidze, D. (2020). The wolf from Dmanisi and augmented reality: review, implications, and opportunities. *Front. Earth Sci.* 8:131. doi: 10.3389/feart.2020.00131

Bartolini-Lucenti, S., Madurell-Malapeira, J., and Rook, L. (2022). The carnivorans from cava Monticino (Faenza, Italy; Messinian) revisited. *Hist. Biol.* 34, 1458–1470. doi: 10.1080/08912963.2022.2042806

Bartolini-Lucenti, S., and Rook, L. (2021). "*Canis*" *ferox* revisited: diet ecomorphology of some long gone (late Miocene and Pliocene) fossil dogs. *J. Mamm. Evol.* 28, 285–306. doi: 10.1007/s10914-020-09500-1

Bartolini-Lucenti, S. B., Rook, L., and Morales, J. (2018). *Nyctereutes* (Mammalia, Carnivora, Canidae) from Layna and the Eurasian raccoon-dogs: an updated revision. *Riv. Ital. Paleontol. Stratigr.* 124, 597–616. doi: 10.13130/2039-4942/10739

Beaudet, A., Dumoncel, J., Thackeray, J. F., Bruxelles, L., Duployer, B., Tenailleau, C., et al. (2016). Upper third molar internal structural organization and semicircular canal morphology in Plio-Pleistocene south African cercopithecoids. *J. Hum. Evol.* 95, 104–120. doi: 10.1016/j.jhevol.2016.04.004

Berta, A. (1988). Quaternary evolution and biogeography of the large south American Canidae (Mammalia, Carnivora). *Geol. Sci.* 132:149.

Bône, A., Louis, M., Martin, B., and Durrleman, S. (2018). "Deformetrica 4: an open-source software for statistical shape analysis" in *Shape in medical imaging. Shape MI 2018*. eds. M. Reuter, C. Wachinger, H. Lombaert, B. Paniagua, M. Lüthi and B. Egger (Cham: Springer), 3–13.

Boudadi-Maligne, M. (2010). Les Canis pleistocenes du sud de la France: approche biosystematique, evolutive et biochronologique. Available at: https://tel.archives-ouvertes.fr/tel-00908031/ (Accessed April 21, 2023).

Chen, L., and Zhang, H. (2012). The complete mitochondrial genome and phylogenetic analysis of *Nyctereutes procyonoides*. *Acta Ecol. Sin.* 32, 232–239. doi: 10.1016/j.chnaes.2012.07.003

Cope, E. D. (1892). A hyena and other Carnivora from Texas. *Am. Nat.* 26, 1028–1029.

Curtis, A. A. (2014). A three-dimensional quantitative investigation of frontal sinus morphology and function in mammalian carnivores. Available at: https://escholarship.org/uc/item/2ts7c0b1 (Accessed April 21, 2023).

Curtis, A. A., Orke, M., Tetradis, S., and Van Valkenburgh, B. (2018). Diet-related differences in craniodental morphology between captive-reared and wild coyotes, *Canis latrans* (Carnivora: Canidae). *Biol. J. Linnean Soc.* 123, 677–693. doi: 10.1093/biolinnean/blx161

Curtis, A. A., and Van Valkenburgh, B. (2014). Beyond the sniffer: frontal sinuses in carnivora. *Anat. Rec.* 297, 2047–2064. doi: 10.1002/ar.23025

De Bonis, L., Peigné, S., Likius, A., Mackaye, H. T., Vignaud, P., and Brunet, M. (2007). The oldest African fox (Vulpes riffautae n. sp., Canidae, Carnivora) recovered in late Miocene deposits of the Djurab desert, Chad. *Naturwissenschaften* 94, 575–580. doi: 10.1007/s00114-007-0230-6

Del Campana, D. (1913). Cani pliocenici della Toscana. *Palaeontogr. Ital.* 19, 189–254.

Dice, L.R. (1917). *Systematic position of several American Tertiary lagomorphs*. Berkeley, CA: University of California Press

Durrleman, S., Pennec, X., Trouvé, A., Ayache, N., and Braga, J. (2012). Comparison of the endocranial ontogenies between chimpanzees and bonobos via temporal regression and spatiotemporal registration. *J. Hum. Evol.* 62, 74–88. doi: 10.1016/j.jhevol.2011.10.004

Durrleman, S., Prastawa, M., Charon, N., Korenberg, J. R., Joshi, S., Gerig, G., et al. (2014). Morphometry of anatomical shape complexes with dense deformations and sparse parameters. *NeuroImage* 101, 35–49. doi: 10.1016/j.neuroimage.2014.06.043

von Waldheim, G. F. (1809). Sur l'*Elasmotherium* et le *Trogontherium*, deux animaux fossils et inconnus de la Russie. *Memoirs de l'Academie Imperiale des Sciences de Moscou* 2, 250–268.

Forsyth-Major, C. I. (1877). Considerazioni sulla fauna dei mammiferi pliocenici e post-pliocenici della Toscana. *Atti Soc. Tosc. Sci. Nat. Mem.* 3, 207–227.

Fostowicz-Frelik, Ł. (2008). First record of *Trogontherium cuvieri* (Mammalia, Rodentia) from the middle Pleistocene of Poland and review of the species. *Geodiversitas* 30, 765–778.

Fox, J., and Weisberg, S. (2019). *An R companion to applied regression*, *3rd*. Sage, Thousand Oaks CA

Garrido, G., and Arribas, A. (2008). *Canis accitanus* nov. sp., a new small dog (Canidae, Carnivora, Mammalia) from the Fonelas P-1 Plio-Pleistocene site (Guadix basin, Granada, Spain). *Geobios* 41, 751–761. doi: 10.1016/j.geobios.2008.05.002

Glaunès, J. A., and Joshi, S. (2006). "Template estimation form unlabeled point set data and surfaces for computational anatomy" in *MICCAI 2006 workshop proceedings. MFCA'06 workshop. Mathematical foundations of computational anatomy: Geometrical and statistical methods for modelling biological shape variability*. eds. X. Pennec and S. Joshi (Copenhagen: INRIA/MICCAI), 29–39.

Hemprich, F. G., and Ehrenberg, C. G. (1828/1834). "Symbolae Physicae" in *Seu Icones et Descriptiones Corporum Naturalium Novorum aut minus Cognitorum quae ex Itineribus per Libyam, Aegyptium, Nubiam, Dongalam, Syriam, Arabiam et Habessiniam, pars Zoologica II, Anima* (Berlin: Officina Academica).

Hugueney, M. (2004). Large rodents from the upper Pliocene of saint-Vallier (Drôme, France): Castoridae, Hystricidae (Mammalia, Rodentia). *Geobios* 37, S126–S132. doi: 10.1016/S0016-6995(04)80012-3

Hugueney, M., Guérin, C., and Poidevin, J.-L. (1989). Découverte de *Trogontherium minus* Newton, 1890 (Rodentia: Castoridae) dans le Villafranchien inférieur de Perrier-Étouaires (Puy-de-Dôme, France): implications phylogénétiques. *Comptes Rendus de l'Académie des Sciences, série II* 309, 763–768.

Huxley, T. H. (1880). On the cranial and dental characters of the Canidæ. *Proc. Zool. Soc. London* 48, 238–288. doi: 10.1111/j.1469-7998.1880.tb06558.x

Joeckel, R. M. (1998). Unique frontal sinuses in fossil and living hyaenidae (Mammalia, Carnivora): description and interpretation. *J. Vertebr. Paleontol.* 18, 627–639. doi: 10.1080/02724634.1998.10011089

Kingdon, J. (1989). *Island Africa: The evolution of Africa's rare plants and animals*, Princeton, NJ: Princeton University Press. ISBN 0–691–08560-9.

Kretzoi, M. (1938). Die Raubtiere von Gombaszög nebst einer Übersicht der Gesamtfauna. *Ann. Musei Natl. Hungarici Pars Mineral. Geol. Palaeontol.* 31, 88–157.

Leidy, J. (1858). Notice of remains of extinct Vertebrata, from the valley of the Niobrara River, collected during the exploring expedition of 1857, in Nebraska, under the command of Lieut. G. K. Warren, U.S. top. Eng., by Dr. F. V. Hayden, geologist to the expedition. *Proc. Acad. Nat. Sci. Philadelphia* 1858, 20–29.

Lindblad-Toh, K., Wade, C. M., Mikkelsen, T. S., Karlsson, E. K., Jaffe, D. B., Kamal, M., et al. (2005). Genome sequence, comparative analysis and haplotype structure of the domestic dog. *Nature* 438, 803–819. doi: 10.1038/nature04338

Lilljeborg, W. (1874). *Fauna Ofver Sveriges och Norges Ryg- gradsdjur I. Daggdjuren*. Uppsala: W. Schultz.

Linnaeus, C. (1758). *Systema Naturae per regna Tria Naturae, Secundum classes, ordines, genera, species, cum Characteribus, Differentiis. Synonymis, Locis. Tomus I. Editio Decima, Reformata* Stockholm: Laurentius Salvius

Linnaeus, C. (1768). *Systema naturae per regna tria naturae, secundum classes, ordines, genera, species, cum characteribus, differentiis synonymis, locis. Regum animale. Class I, Mammalia. 12th*. Stockholm: Laurentius Salvius.

López Martínez, N. (1977). Nuevos lagomorfos (Mamma- lia) del Terciario y Cuaternario de España. *Trab Neógeno-Cuaternario* 8, 7–45.

López-Martínez, N. (1989) Revisión sistemática y bioestratigráfica de los Lagomorpha (Mammalia) del Terciario y Cuaternario inferior de España. PhD Univ. Madrid 1977, published in mem. Museo Paleont., Univ. Zaragoza, Madrid.

Lopez-Martinez, N. (2008). "The Lagomorph Fossil Record and the Origin of the European Rabbit," in *Lagomorph Biology*, eds. P. C. Alves, N. Ferrand and K. Hackländer (Berlin, Heidelberg: Springer-Verlag Berlin Heidelberg), 27–46

Lyras, G., and Van Der Geer, A. (2006). Adaptations of the Pleistocene Island canid *Cynotherium sardous* (Sardinia, Italy) for hunting small prey. *Cranium* 23, 51–60.

Lyras, G. A., van der Geer, A. A. E., Dermitzakis, M. D., and De Vos, J. (2006). *Cynotherium sardous*, an insular canid (Mammalia: Carnivora) from the Pleistocene of Sardinia (Italy), and its origin. *J. Vertebr. Paleontol.* 26, 735–745. doi: 10.1671/0272-4634(2006)26[735:CSAICM]2.0.CO;2

Madurell-Malapeira, J., Palombo, M. R., and Sotnikova, M. (2015). *Cynotherium malatestai*, sp. nov. (Carnivora, Canidae) from the early middle Pleistocene deposits of Grotta dei Fiori (Sardinia, Western Mediterranean). *1. J. Vertebr. Paleontol.* 35:e943400. doi: 10.1080/02724634.2014.943400

Marciszak, A., Kropczyk, A., and Lipecki, G. (2021). The first record of *Cuon alpinus* (Pallas, 1811) from Poland and the possible impact of other large canids on the evolution of the species. *J. Quat. Sci.* 36, 1101–1121. doi: 10.1002/jqs.3340

Maridet, O., Escarguel, G., Costeur, L., Mein, P., Hugueney, M., and Legendre, S. (2007). Small mammal (rodents and lagomorphs) European biogeography from the late Oligocene to the mid Pliocene. *Glob. Ecol. Biogeogr.* 16, 529–544. doi: 10.1111/j.1466-8238.2006.00306.x

Martin, R. (1973). Trois nouvelles especes de Caninae (Canidae, Carnivora) des gisements plio-villafranchiens d'Europe. *Doc. des Lab Géologie la Fac. des Sci. Lyon* 57, 87–96.

Martínez-Navarro, B., Gossa, T., Carotenuto, F., Bartolini-Lucenti, S., Palmqvist, P., Asrat, A., et al. (2023). The earliest Ethiopian wolf: implications for the species evolution and its future survival. *Commun. Biol.* 6:350. doi: 10.1038/s42003-023-04908-w

Matthew, W. D. (1918). Contributions to the Snake Creek Fauna. *Bull. Am. Mus. Nat. Hist.* 38, 183–229.

Matthew, W. D. (1924). Third contribution to the Snake Creek fauna. *Bull. Am. Mus. Nat. Hist.* 50, 59–210.

McGreevy, P., Grassi, T. D., and Harman, A. M. (2004). A strong correlation exists between the distribution of retinal ganglion cells and nose length in the dog. *Brain. Behav. Evol.* 63, 13–22. doi: 10.1159/000073756

Mein, P., and Aymar, J. (1984). Decouvertes recentes de mammiferes dans le Pliocene du Roussillon. Note preliminaire. *Publications du Mus. Confluences* 22, 69–71.

Merriam, C.H. (1888). *Description of a new fox from Southern California: Vulpes macrotis sp. nov. long-eared fox*. Gibson Bros.

Merriam, J. C. (1911). Tertiary mammal beds of Virgin Valley and Thousand Creek in north-western Nevada. Part 2. Vertebrate faunas. *Bull. Depart. Geol. Univ. Califor.* 11, 199–304.

Miller, W. E., and Carranza-Castañeda, O. (1998). Late tertiary canids from Central Mexico. *J. Paleontol.* 72, 546–556. doi: 10.1017/S002233600002432X

Montoya, P., Morales, J., and Abella, J. (2009). Eucyon debonisi n. sp., a new Canidae (Mammalia, Carnivora) from the latest Miocene of Venta del Moro (Valencia, Spain). *Geodiversitas* 31, 709–722. doi: 10.5252/g2009n4a709

Morales, J., Pickford, M., and Soria, D. (2005). Carnivores From the Late Miocene and Basal Pliocene of the Tugen Hills, Kenya. *Rev. la Soc. Geol. Espana* 18, 39–61.

Newton, E. T. (1890). On some new mammals from the red and Norwich crags. *Quart. J. Geol. Soc. London* 46, 444–453. doi: 10.1144/GSL.JGS.1890.046.01-04.29

Nomade, S., Pastre, J. F., Guillou, H., Faure, M., Guérin, C., Delson, E., et al. (2014). 40Ar/39Ar constraints on some French landmark late Pliocene to early Pleistocene large mammalian paleofaunas: paleoenvironmental and paleoecological implications. *Quat. Geochronol.* 21, 2–15. doi: 10.1016/j.quageo.2012.12.006

Odintzov, I. A. (1967). New species of Pliocene Carnivora, *Vulpes odessana* sp. nov. from the karst cave of Odessa. *Paleontolog Sbornik, L'vov University* 4, 130–137. (in Russian)

Paulli, S. (1900). Über die Pneumaticität des Schädels bei den Säugetieren. Eine morphologische Studie III. Über die Morphologie des Siebbeins und Pneumaticität bei den Insectivoren, Hyracoideen, Chiropteren, Carnivoren, Pinnipedien, Edentates, Rodentiern, Prosimien und Primaten. *Gegenbaurs Morphologisches Jahrbuch* 28, 483–564.

Pei, W. (1934). On the Carnivora from locality 1 of Choukoutien. *Palaeontol. Sin. Ser. C* 8, 1–216.

Pérez-Ramos, A., Tseng, Z. J., Grandal-D'Anglade, A., Rabeder, G., Pastor, F. J., and Figueirido, B. (2020). Biomechanical simulations reveal a trade-off between adaptation to glacial climate and dietary niche versatility in European cave bears. *Sci. Adv.* 6:eaay9462. doi: 10.1126/sciadv.aay9462

Perri, A. R., Mitchell, K. J., Mouton, A., Álvarez-Carretero, S., Hulme-Beaman, A., Haile, J., et al. (2021). Dire wolves were the last of an ancient New World canid lineage. *Nature* 591, 87–91. doi: 10.1038/s41586-020-03082-x

Qiu, Z., Deng, T., and Wang, B. (2004). Early Pleistocene mammalian fauna from Longdan, Dongxiang, Gansu, China. *Paleontol. Sin.* 27:198.

Qiu, Z., Huang, W.-L., and Cuo, Z.-H. (1979). Hyaenidae of the Qingyang (K'ingyang) *Hipparion* fauna. *Vertebr. Palasiat.* 17, 200–221.

R Core Team (2021). *R: A language and environment for statistical computing*. R Foundation for Statistical Computing, Vienna, Austria

Radulesco, C., and Samson, P. (1967). Contribution à la connaissance du complexe faunistique de Malusteni-Beresti (Pléistocène inférieur), Roumanie I. Ord. Lagomorpha, Fam. Leporidae. Neues Jahrb. für Mineral. Geol. und Paläontologie. *Monatshefte* 9, 544–563.

Rook, L. (1992). "*Canis*" *monticinensis* sp. nov., a new Canidae (Carnivora, Mammalia) from the late Messinian of Italy. *Boll. della Soc. Paleontol. Ital.* 31, 151–156.

Rook, L. (2009). The wide-ranging genus *Eucyon* Tedford & Qiu, 1996 (Mammalia, Carnivora, Canidae, Canini) in the Mio-Pliocene of the Old World. *Geodiversitas* 31, 723–741. doi: 10.5252/g2009n4a723

Rook, L., Bartolini-Lucenti, S., Cirilli, O., Delfino, M., Ferretti, M. P., and Pando, L. (2023). "Vertebrate records," in *Reference Module in Earth Systems and Environmental Sciences*. (Elsevier Inc.), 1–11.

RStudio Team (2021). *RStudio: Integrated development environment for R*. RStudio, PBC, Boston, MA

Ruiz, J. V., Ferreira, G. S., Lautenschlager, S., de Castro, M. C., and Montefeltro, F. C. (2023). Different, but the same: inferring the hunting behaviour of the hypercarnivorous bush dog (*Speothos venaticus*) through finite element analysis. *J. Anat.* 242, 553–567. doi: 10.1111/joa.13804

Rüppell, E. (1835/1840). *Neue Wirbelthiere zu der Fauna von Abyssinien gehorig. Saugethiere*. Siegmund Schmerber, Frankfurt am Main

Rüppell, E. (1842). Saugethiere aus der Ordnung der Nager, beo- bachtet in Nordostlichen Africa. *Mus. Senckenbergianum* 3, 99–116.

Say, T. (1823). Account of an expedition from Pittsburgh to the Rocky Mountains, performed in the years 1819 and '20, by order of the hon. J. C. Calhoun, Sec'y of war: under the command of Major Stephen H. long. From the notes of Major long, Mr. T. Say, and other gentlemen of the exploring party, ed. E. James (Philadelphia, PA: H.C. Carey and I. Lea), 503.

Schlager, S. (2017). "Morpho and Rvcg e shape analysis in R: R-packages for geometric morphometrics, shape analysis and surface manipulations" in *Statistical Shape and Deformation Analysis, Methods, Implementation and Applications*. eds. G. Zheng, S. Li and G. Székely (London: Academic Press), 217–256.

Schreber, J. C. D. (1775). *Die Säugethiere in Abbildungen nach der Natur mit Beschreibungen*. Erlangen: Wolfgang Walther.

Slater, G. J., Dumont, E. R., and Van Valkenburgh, B. (2009). Implications of predatory specialization for cranial form and function in canids. *J. Zool.* 278, 181–188. doi: 10.1111/j.1469-7998.2009.00567.x

Smith, C. H. (1839). "The canine family in general or the genus *Canis*" in *The naturalist's library, vol. 18. Natural history of dogs*. ed. W. Jardine, vol. *1* (Edinburgh: W. H. Lizars), 267.

Soergel, W. (1925). Die Säugetierfauna des altdiluvialen Tonlages von Jockgrim. *Pfalz. Zeits. Deut. Geol. Ges.* 77, 405–438.

Sotnikova, M.V. (1989). The carnivore mammals from the Pliocene to the Early Pleistocene. Stratigraphic significance. *Trans. Geol Inst RAS* 440, 1–122. (in russian)

Sotnikova, M. (2006). A new canid *Nurocyon chonokhariensis* gen. et sp. nov. (Canini, Canidae, Mammalia) from the Pliocene of Mongolia. *CFS Cour. Forschungsinstitut Senckenb.*, 11–21.

Sotnikova, M., and Rook, L. (2010). Dispersal of the Canini (Mammalia, Canidae: Caninae) across Eurasia during the late Miocene to early Pleistocene. *Quat. Int.* 212, 86–97. doi: 10.1016/j.quaint.2009.06.008

Spassov, N., and Rook, L. (2006). *Eucyon marinae* sp. nov. (Mammalia, Carnivora), a new canid species from the Pliocene of Mongolia, with a review of forms referable to the genus. *Riv. Ital. di Paleontol. e Stratigr.* 112, 123–133.

Stiner, M. C., Howell, F. C., Martínez-Navarro, B., Tchernov, E., and Bar-Yosef, O. (2001). Outside Africs: middle Pleistocene *Lycaon* from Hayonim cave, Israel. *Boll. della Soc. Paleontol. Ital.* 40, 293–302.

Studiati, C. (1857) "Description des fossiles de la brèche osseuse de Monreale de Bonaria près de Cagliari", in *Voyage en Sardeigne 3*, ed. MarmoraA. La, Turin: Arthus Bertrand, 651–704.

Sundevall, C. J. (1847). Nya Mammalia från Sydafrika. *Ofv. K. Svenska Vet.-Akad. Forhandl. Stockholm* 3, 118–121.

Tamvakis, A., Savvidou, A., Spassov, N., Youlatos, D., Merceron, G., and Kostopoulos, D. S. (2022). New insights on early Pleistocene *Nyctereutes* from the Balkans based on material from Dafnero-3 (Greece) and Varshets (Bulgaria). *Palaeoworld* 3. doi: 10.1016/j.palwor.2022.09.006

Tedford, R. H., and Qiu, Z. (1996). A new canid genus from the Pliocene of Yushe, Shanxi Province. *Vertebr. Palasiat.* 34, 27–40.

Tedford, R. H., Taylor, B. E., and Wang, X. (1995). Phylogeny of Caninae (Carnivora: Canidae): the living taxa. *Am. Museum Novit.* 3146, 1–40.

Tedford, R. H., Wang, X., and Taylor, B. E. (2009). Phylogenetic systematics of the north American fossil Caninae (Carnivora: Canidae). *Bull. Am. Museum Nat. Hist.* 325, 1–218. doi: 10.1206/574.1

Teilhard de Chardin, P. (1940). The fossils from locality 18 near Peking. *Palaeontol. Sin. Ser. C* 9, 1–95.

Teilhard De Chardin, P., and Piveteau, J. (1930). Les mammifères fossiles de Nihowan (Chine). *Ann. Paleontol.* 19, 1–134.

Temminck, C. J. (1820). Sur le genre Hyène, et description d'une espèce nouvelle, découverte en Afrique. *Ann. Gen. Sci. Phys.* 3, 46–57.

Tseng, Z. J., and Wang, X. (2010). Cranial functional morphology of fossil dogs and adaptation for durophagy in *Borophagus* and *Epicyon* (Carnivora, Mammalia). *J. Morphol.* 271, 1386–1398. doi: 10.1002/jmor.10881

Urciuoli, A., Zanolli, C., Beaudet, A., Dumoncel, J., Santos, F., Moyà-Solà, S., et al. (2020). The evolution of the vestibular apparatus in apes and humans. *elife* 9:e51261. doi: 10.7554/eLife.51261

Valenciano, A., Morales, J., and Govender, R. (2022). *Eucyon khoikhoi* sp. nov. (Carnivora: Canidae) from Langebaanweg "E" quarry (early Pliocene, South Africa): the most complete African canini from the Mio-Pliocene. *Zool. J. Linnean Soc.* 194, 366–394. doi: 10.1093/zoolinnean/zlab022

Van Valkenburgh, B. (1990). "Skeletal and dental predictors ofbodymass in carnivores" in *Body size in mammalian Paleobiology: Estimation and biological implications*. eds. J. Damuth and B. MacFadden (Cambridge: Cambridge University Press), 181–205.

Van Valkenburgh, B., and Koepfli, K.-P. (1993). Cranial and dental adaptations to predation in canids. *Symp. Zool. Soc. London* 65, 15–37.

Van Valkenburgh, B., Sacco, T., and Wang, X. (2003). Pack hunting in Miocene borophagine dogs: evidence from craniodental morphology and body size. *Vertebr. Foss. Their Context Contrib. Honor Richard H. Tedford*. 279, 147–162.

Vinuesa, V. (2018). Bone-cracking hyenas (Carnivora, Hyaenidae) from the European Neogene and quaternary: taxonomy. *Paleobiol. Evolut.* Unpublished PhD Thesis

Vinuesa, V., Iurino, D. A., Madurell-Malapeira, J., Liu, J., Fortuny, J., Sardella, R., et al. (2016). Inferences of social behavior in bone-cracking hyaenids (Carnivora, Hyaenidae) based on digital paleoneurological techniques: implications for human–carnivoran interactions in the Pleistocene. *Quat. Int.* 413, 7–14. doi: 10.1016/j.quaint.2015.10.037

Vinuesa, V., Madurell-Malapeira, J., Fortuny, J., and Alba, D. M. (2015). The Endocranial morphology of the Plio-Pleistocene bone-cracking hyena *Pliocrocuta perrieri*: behavioral implications. *J. Mamm. Evol.* 22, 421–434. doi: 10.1007/s10914-015-9287-8

Wang, X. (1994). Phylogenetic systematics of the Hesperocyoninae (Carnivora, Canidae). *Bull. Am. Museum Nat. Hist.* 221, 1–207.

Wang, X., and Tedford, R. H. (2008). *Dogs and their fossil relatives*. New York: Columbia University Press

Wang, X., Tedford, R. H., and Taylor, B. E. (1999). Phylogenetic systematics of the Borophaginae (Carnivora. Canidae). *Bull. Am. Mus. Nat. Hist.* 243, 1–391.

Wayne, R. K., and Ostrander, E. A. (2007). Lessons learned from the dog genome. *Trends Genet.* 23, 557–567. doi: 10.1016/j.tig.2007.08.013

Werdelin, L. (1989). Constraint and adaptation in the bone-cracking canid *Osteoborus* (Mammalia: Canidae). *Paleobiology* 15, 387–401. doi: 10.1017/S009483730000957X

Werdelin, L., Lewis, M. E., and Haile-Selassie, Y. (2015). A critical review of African species of *Eucyon* (Mammalia; Carnivora; Canidae), with a new species from the Pliocene of the Woranso-mille area, Afar region, Ethiopia. *Pap. Palaeontol.* 1, 33–40. doi: 10.1002/spp2.1001

Werdelin, L., and Sanders, W. J. (2010). *Cenozoic Mammals of Africa*. Berkeley: University of California Press.

Yalden, D. W. (1985). Tachyoryctes macrocephalus. *Mamm. Species* 237, 1–3. doi: 10.2307/3503827

Zanolli, C., Kaifu, Y., Pan, L., Xing, S., Mijares, A., Kullmer, O., et al. (2022). Further analyses of the structural organization of *Homo luzonensis* teeth: evolutionary implications. *J. Hum. Evol.* 163:103124. doi: 10.1016/j.jhevol.2021.103124

Zrzavý, J., Duda, P., Robovský, J., Okřinová, I., and Pavelková Řičánková, V. (2018). Phylogeny of the Caninae (Carnivora): combining morphology, behaviour, genes and fossils. *Zool. Scr.* 47, 373–389. doi: 10.1111/zsc.12293